A Color Out of Space

‘Oumuamua’s Brief and Mysterious Visit to the Solar System

Gregory Laughlin
Yale University

Darryl Seligman
Yale University

Konstantin Batygin
Caltech

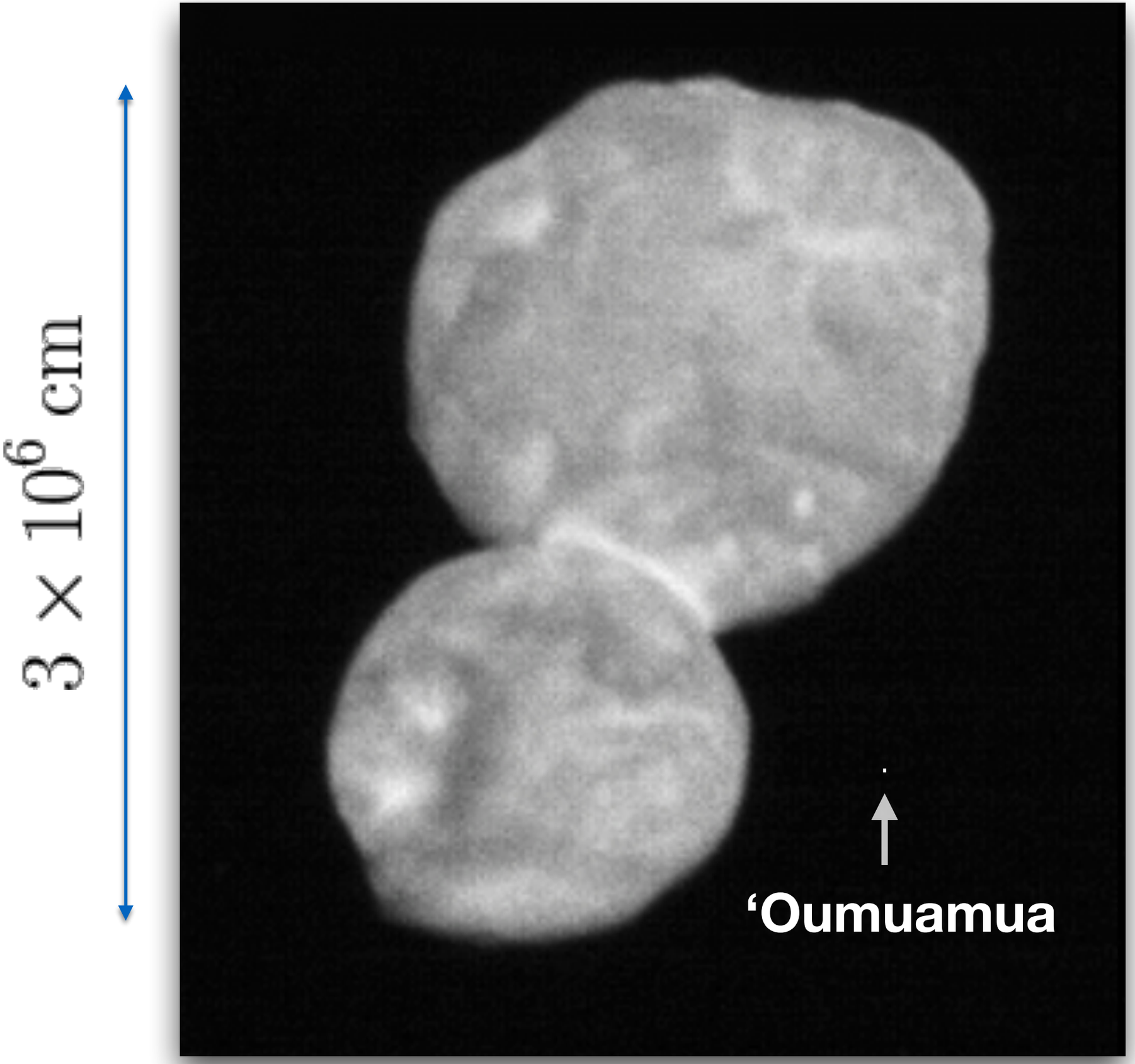
3×10^6 cm
'Oumuamua

M.P.E.C. 2017-U181 Issued 2017 Oct. 25, 03:53 UT ← 03:53 UTC

07:53 PM PDT

The Minor Planet Electronic Circulars contain information on unusual minor planets and routine data on comets. They are published on behalf of Division F of the International Astronomical Union by the Minor Planet Center, Smithsonian Astrophysical Observatory, Cambridge, MA 02138, U.S.A.

Prepared using the Tamkin Foundation Computer Network

MPC@CFA.HARVARD.EDU
URL http://www.minorplanetcenter.net/ ISSN 1523-6714

COMET C/2017 U1 (PANSTARRS)

Further observations of this object are very much desired. Unless there are serious problems with much of the astrometry listed below, strongly hyperbolic orbits are the only viable solutions. Although it is probably not too sensible to compute meaningful original and future barycentric orbits, given the very short arc of observations, the orbit below has e ~ 1.2 for both values. If further observations confirm the unusual nature of this orbit, this object may be the first clear case of an interstellar comet.

Observations:

```
CK17U010  C2017 10 18.47298 01 59 57.442+02 06 04.30          19.8 TLEU181F51
CK17U010  C2017 10 18.49990 01 59 08.910+02 07 20.19               LEU181F51
CK17U010  C2017 10 19.39715 01 34 55.362+02 45 03.20          19.9 TLEU181F51
CK17U010  C2017 10 19.40837 01 34 38.745+02 45 28.24          19.9 TLEU181F51
CK17U010  C2017 10 19.41968 01 34 21.948+02 45 53.55          20.1 TLEU181F51
CK17U010  C2017 10 19.43106 01 34 05.174+02 46 18.89          20.1 TLEU181F51
CK17U010 KC2017 10 19.86072 01 24 07.89 +03 01 07.5           19.6 TUEU181104
CK17U010 KC2017 10 19.86492 01 24 02.21 +03 01 16.3           19.8 TUEU181104
CK17U010 KC2017 10 19.86905 01 23 56.69 +03 01 24.7           20.3 TUEU181104
CK17U010 KC2017 10 19.94093401 22 22.288+03 03 53.76          20.3 TUEU181J04
CK17U010 KC2017 10 19.94390101 22 18.372+03 03 59.57          20.1 TUEU181J04
CK17U010  C2017 10 20.17250 01 17 27.47 +03 11 07.8           19.9 TUEU181I52
CK17U010  C2017 10 20.17348 01 17 26.22 +03 11 09.6           20.2 TUEU181I52
CK17U010  C2017 10 20.17448 01 17 24.96 +03 11 11.3           20.2 TUEU181I52
CK17U010  C2017 10 20.17546 01 17 23.73 +03 11 13.0           20.6 TUEU181I52
CK17U010 KC2017 10 21.22371 00 57 56.30 +03 39 16.9           20.2 ToEU181291
CK17U010 KC2017 10 21.22623 00 57 53.76 +03 39 20.5           19.5 ToEU181291
CK17U010 KC2017 10 21.22877 00 57 51.19 +03 39 24.2           19.6 ToEU181291
CK17U010  C2017 10 21.37476 00 55 26.71 +03 42 45.0           20.4 ToEU181926
CK17U010  C2017 10 21.37804 00 55 23.53 +03 42 49.8           20.1 ToEU181926
CK17U010  C2017 10 21.38132 00 55 20.35 +03 42 53.7           20.4 ToEU181926
CK17U010 |C2017 10 22.29708 00 41 56.27 +04 01 25.0                vEU181H06
```

Observer details:
104 San Marcello Pistoiese. Observers P. Bacci, M. Maestripieri. Measurers
P. Bacci, L. Tesi, G. Fagioli. 0.60-m f/4 reflector + CCD.
291 LPL/Spacewatch II. Observer R. A. Mastaler. 1.8-m f/2.7 reflector + CCD.
734 Farpoint Observatory. Observer G. Hug. 0.69-m reflector + CCD.
926 Tenagra II Observatory. Observers M. Schwartz, P. R. Holvorcem. Measurer
M. Schwartz. 0.81-m f/7 Ritchey-Chretien + CCD.
F51 Pan-STARRS 1, Haleakala. Observers J. Bulger, T. Lowe, A. Schultz,
M. Willman. Measurers K. Chambers, S. Chastel, L. Denneau, H. Flewelling,
M. Huber, E. Lilly, E. Magnier, R. Wainscoat, C. Waters, R. Weryk. 1.8-m
Ritchey-Chretien + CCD.
G96 Mt. Lemmon Survey. Observer G. J. Leonard. Measurers E. J. Christensen,
D. C. Fuls, A. R. Gibbs, A. D. Grauer, J. A. Johnson, R. A. Kowalski,
S. M. Larson, G. J. Leonard, R. G. Matheny, R. L. Seaman, F. C. Shelly.
1.5-m reflector + 10K CCD.
H06 iTelescope Observatory, Mayhill. Observer H. Sato. 0.43-m f/6.8
astrograph + CCD + f/4.5 focal reducer.
I52 Steward Observatory, Mt. Lemmon Station. Observer R. A. Kowalski.
Measurers E. J. Christensen, D. C. Fuls, A. R. Gibbs, A. D. Grauer,
J. A. Johnson, R. A. Kowalski, S. M. Larson, G. J. Leonard, R. G. Matheny,
R. L. Seaman, F. C. Shelly. 1.0-m reflector + CCD.
J04 ESA Optical Ground Station, Tenerife. Observer D. Abreu. Measurers
M. Micheli, D. Koschny, M. Busch, A. Knoefel, E. Schwab. 1.0-m f/4.4
reflector + CCD.
Q62 iTelescope Observatory, Siding Spring. Observer H. Sato. 0.51-m f/6.8
astrograph + CCD + f/4.5 focal reducer.

Orbital elements:
C/2017 U1 (PANSTARRS)
Epoch 2017 Sept. 4.0 TT = JDT 2458000.5
T 2017 Sept. 9.41719 TT MPCW

q	0.2515404	(2000.0)	P	Q
z	-0.7541603	Peri. 241.01670	-0.63536548	+0.68733697
+/-	0.0181483	Node 24.61531	+0.49903801	+0.71329677
e	1.1897018	Incl. 122.32770	-0.58929769	-0.13702411

>From 34 observations 2017 Oct. 18-24, mean residual 0".5.

Ephemeris:
C/2017 U1 (PANSTARRS)

Date TT	R. A. (2000)	Decl.	Delta	r	Elong.	Phase	m1	m2
2017 09 25	09 48 43.3	-06 12 59	0.6925	0.5884	34.9	102.8	20.5	
...								
2017 10 10	07 36 11.4	-05 42 56	0.2294	0.9879	80.7	86.0	18.8	
...								
2017 10 18	02 14 50.4	+01 42 29	0.1968	1.1887	166.6	11.2	18.7	

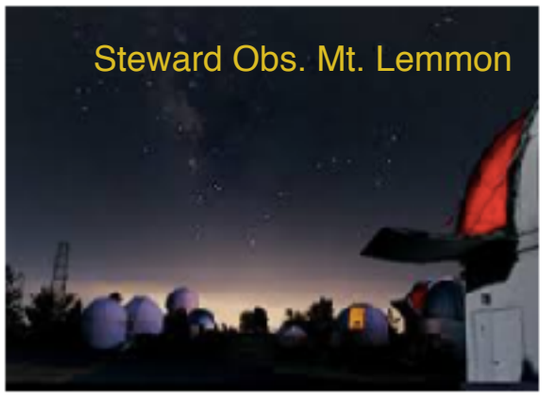


PEGASUS
Nov 1
Dec 1
Jan 1, 2018
Today
Incoming
LYRA
CYGNUS
Outgoing
Solar Apex
July 1, 2016
PISCES
Oct 19
PANSTARRS
Discovery
HERCULES
July 1, 2017
BOOTES
Aug 1
VIRGO
URSA MAJOR
ERIDANUS
Sept 1
ECLIPTIC
Autumn 2017
Path of 'Oumuamua
CANIS MAJOR

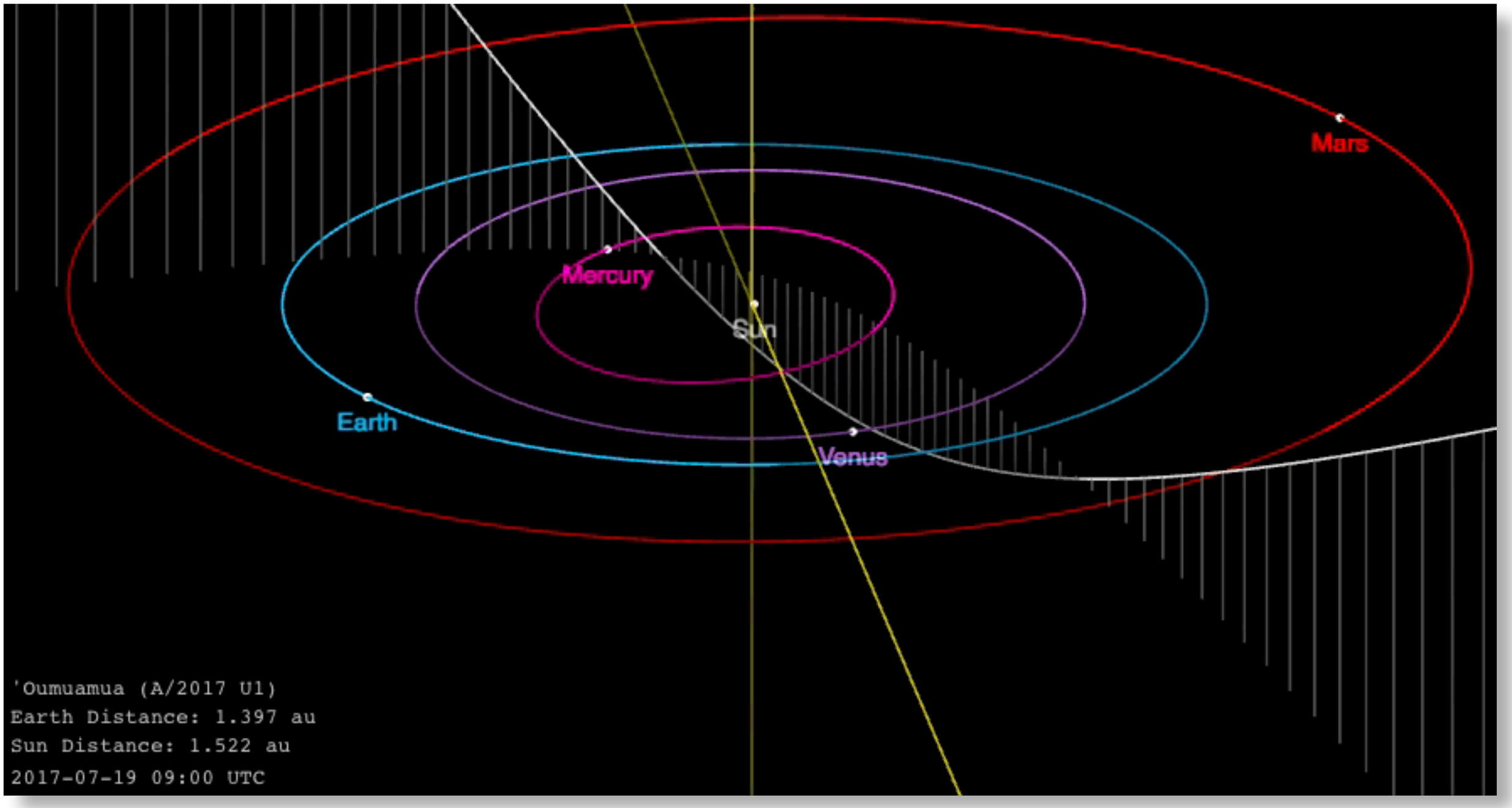

JPL Horizons

Absolute magnitude $$H = m - 2.5 \log_{10} \left(\frac{d_{BS}^2 \, d_{BO}^2}{P(\chi) d_0^4} \right) = 22.4$$

1 AU

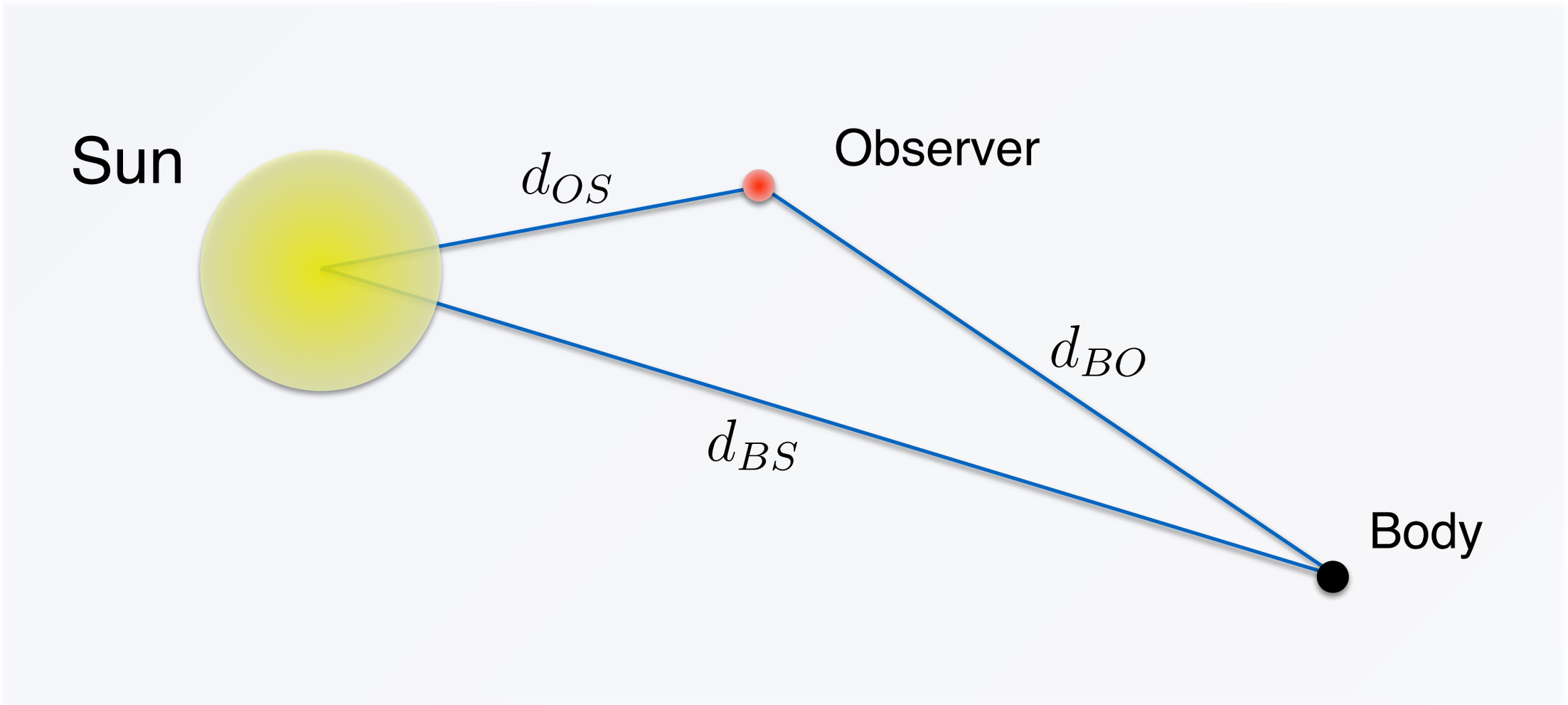

$$\cos \chi = \frac{d_{BO}^2 + d_{BS}^2 - d_{OS}^2}{2 d_{BO} d_{BS}}$$

Phase angle.

Approximation is exact for a diffuse reflecting sphere.

$$P(\chi) \simeq \frac{2}{3} \left((1 - \frac{\chi}{\pi}) \cos \chi + \frac{1}{\pi} \sin \chi \right)$$

Integration of reflected light normalized to a number in the range 0 to 1.

07:53 PM PDT Oct. 24 2017

Palomar 200-inch

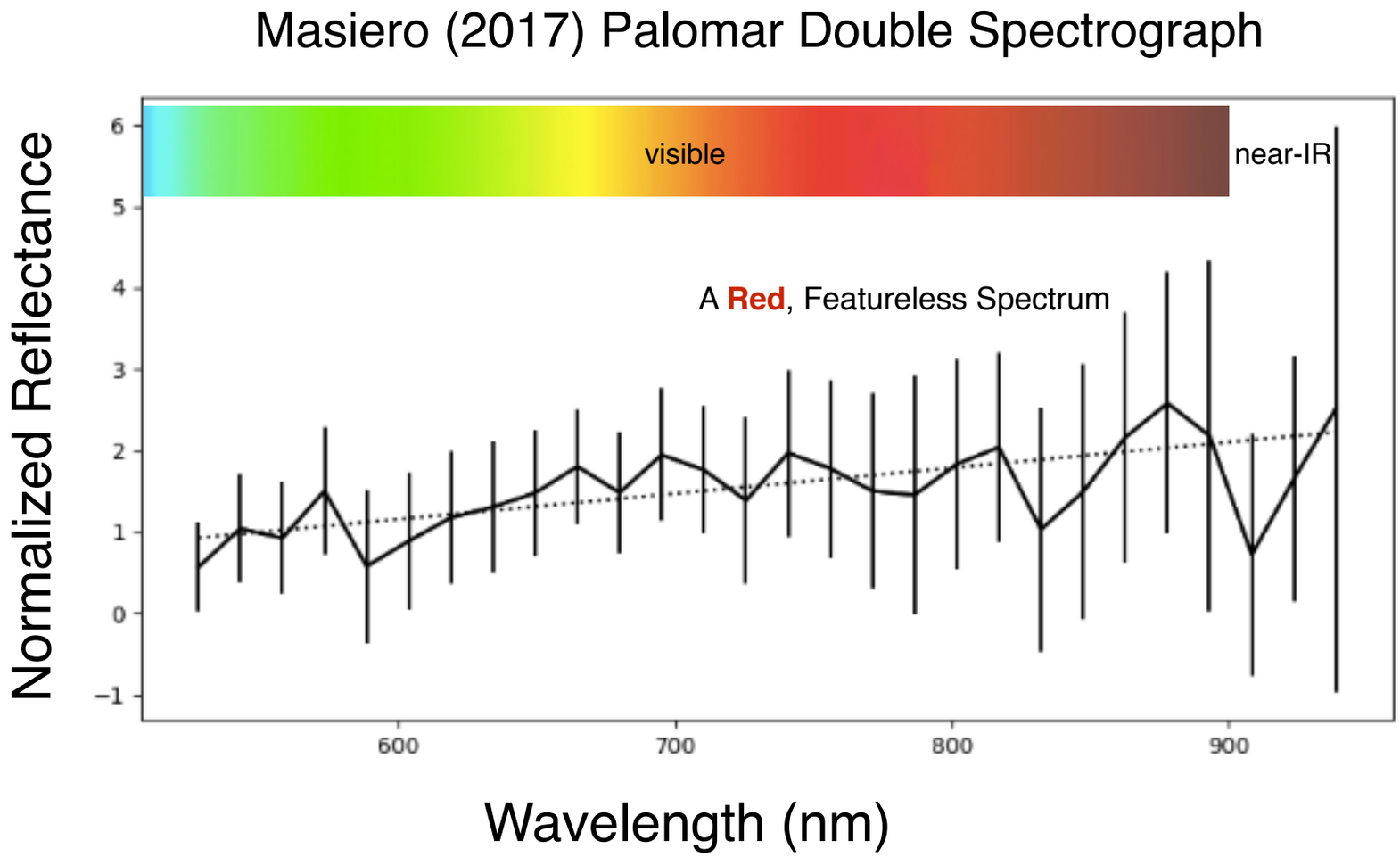

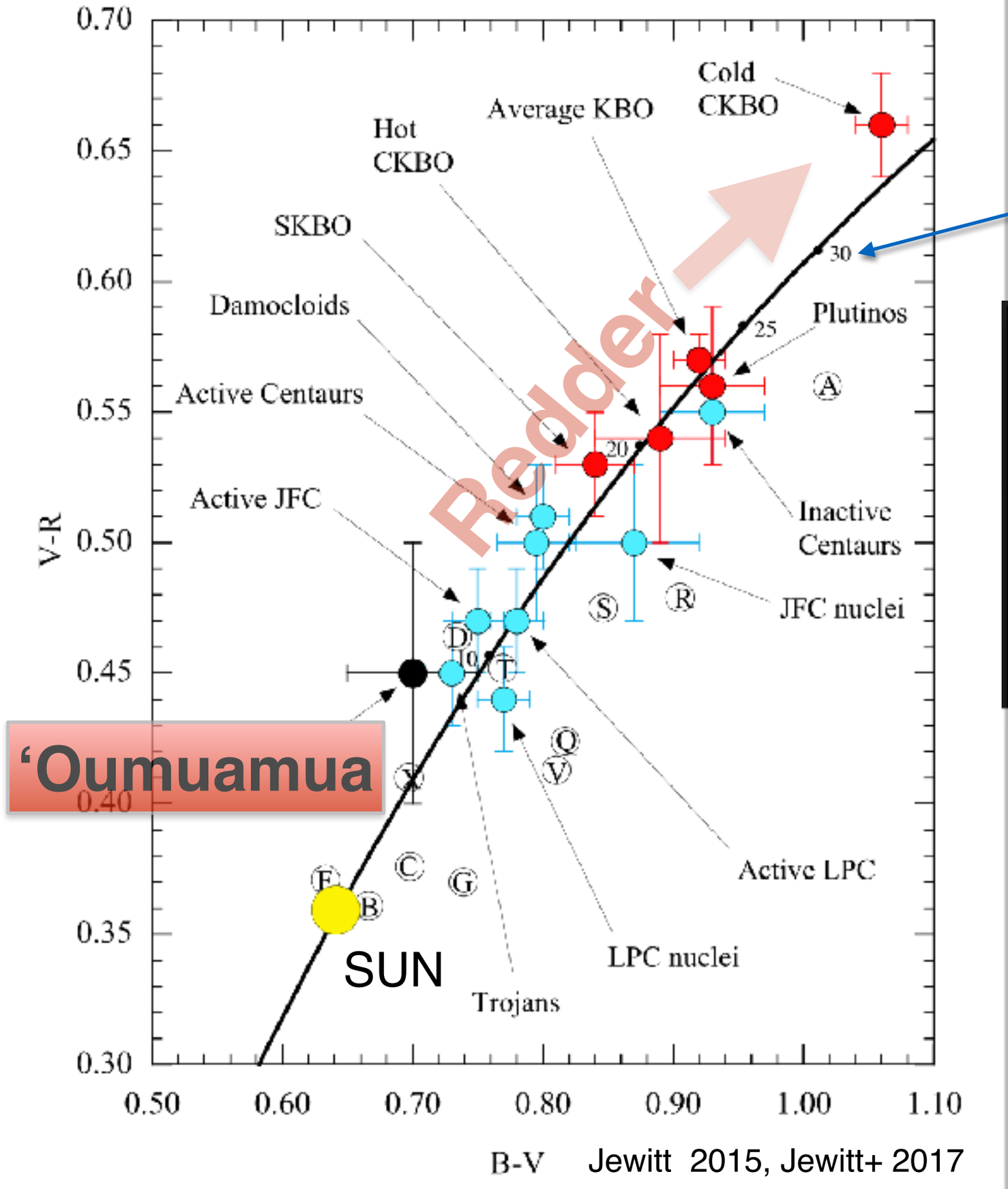

Jewitt 2015, Jewitt+ 2017

Line shows locus of constant spectral gradients, 30=30% slope

Phoebe (typical **dark**, **red** outer solar system object)

Assuming low albedo:

$$d \sim 100 \text{ meters}$$

This contrasts with the Spitzer **non**-detection.

Trilling+2018

MPEC 2017-U183: A/2017 U1

◀ Read *MPEC* 2017-U182 ▶ Read *MPEC* 2017-U184

M.P.E.C. 2017-U183 Issued 2017 Oct. 25, 22:22 UT ← **afternoon in Western Hemisphere**

The Minor Planet Electronic Circulars contain information on unusual minor planets and routine data on comets. They are published on behalf of Division F of the International Astronomical Union by the Minor Planet Center, Smithsonian Astrophysical Observatory, Cambridge, MA 02138, U.S.A.

Prepared using the Tamkin Foundation Computer Network

MPC@CFA.HARVARD.EDU
URL http://www.minorplanetcenter.net/ ISSN 1523-6714

A/2017 U1

K. Meech (Institute of Astronomy, University of Hawaii) reports that in a very deep stacked image, obtained with the VLT, this object appears completely stellar. The prefix for the designation 2017 U1 is therefore being changed to A/, in line with the 1995 IAU Resolution on the system of comet designations.

Observations:

↓ Old astrometry from previous nights

```
AK17U010  C2017 10 18.47298 01 59 57.442+02 06 04.30          19.8 wLEU183F51
AK17U010  C2017 10 18.49990 01 59 08.910+02 07 20.19               LEU183F51
AK17U010  C2017 10 19.39715 01 34 55.362+02 45 03.20          19.9 wLEU183F51
AK17U010  C2017 10 19.40837 01 34 38.745+02 45 28.24          19.9 wLEU183F51
AK17U010  C2017 10 19.41968 01 34 21.948+02 45 53.55          20.1 wLEU183F51
AK17U010  C2017 10 19.43106 01 34 05.174+02 46 18.89          20.1 wLEU183F51
```

↓ **New** astrometry from Oct 25th

```
AK17U010  C2017 10 25.19587 00 12 06.02 +04 40 47.9          21.3 RoEU183926
AK17U010  C2017 10 25.20769 00 12 00.38 +04 40 55.9          21.2 RoEU183926
AK17U010  C2017 10 25.21951 00 11 54.70 +04 41 02.0          21.4 RoEU183926
AK17U010  C2017 10 25.24174 00 11 44.09 +04 41 15.9               UEU183G96
AK17U010  C2017 10 25.24440 00 11 42.76 +04 41 17.8          21.7 GUEU183G96
AK17U010  C2017 10 25.24719 00 11 41.39 +04 41 20.5          22.0 GUEU183G96
AK17U010  C2017 10 25.25007 00 11 39.91 +04 41 23.5               UEU183G96
```

(VLT & GST stacked images)

Rapid fade confers **urgency**!

Light Curve

Photometry redrawn from Meech+ (2017)

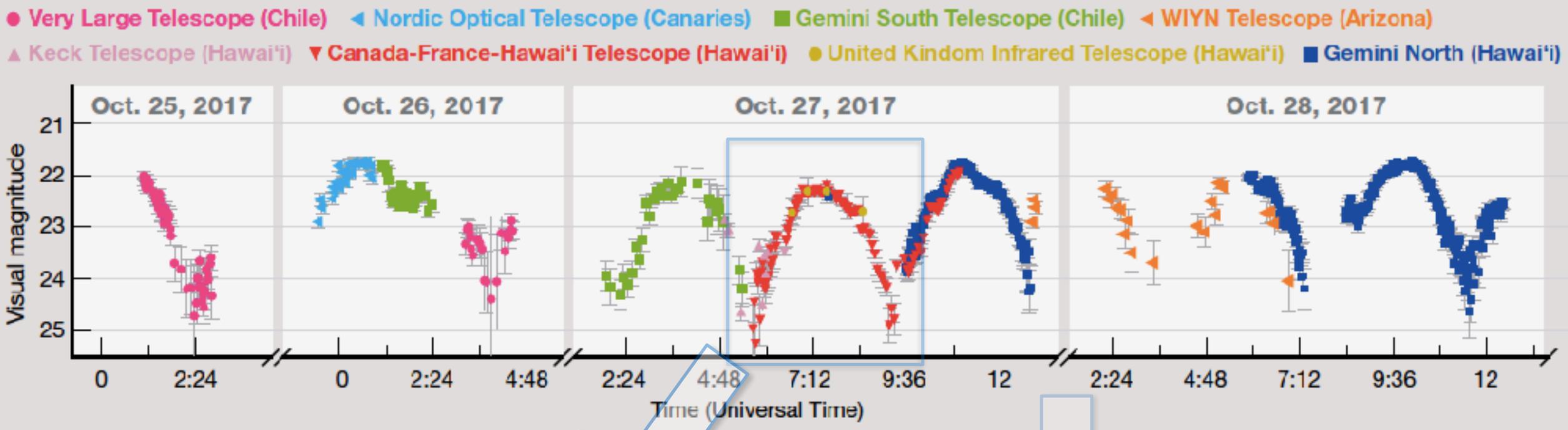

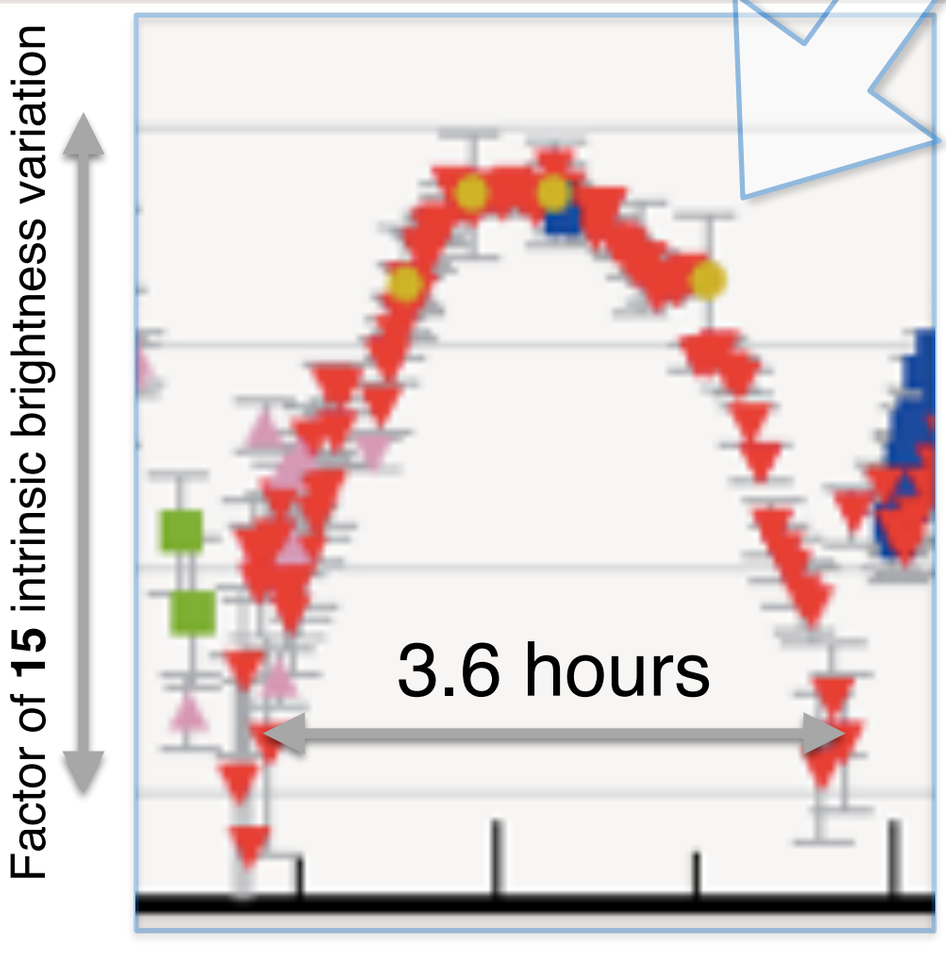

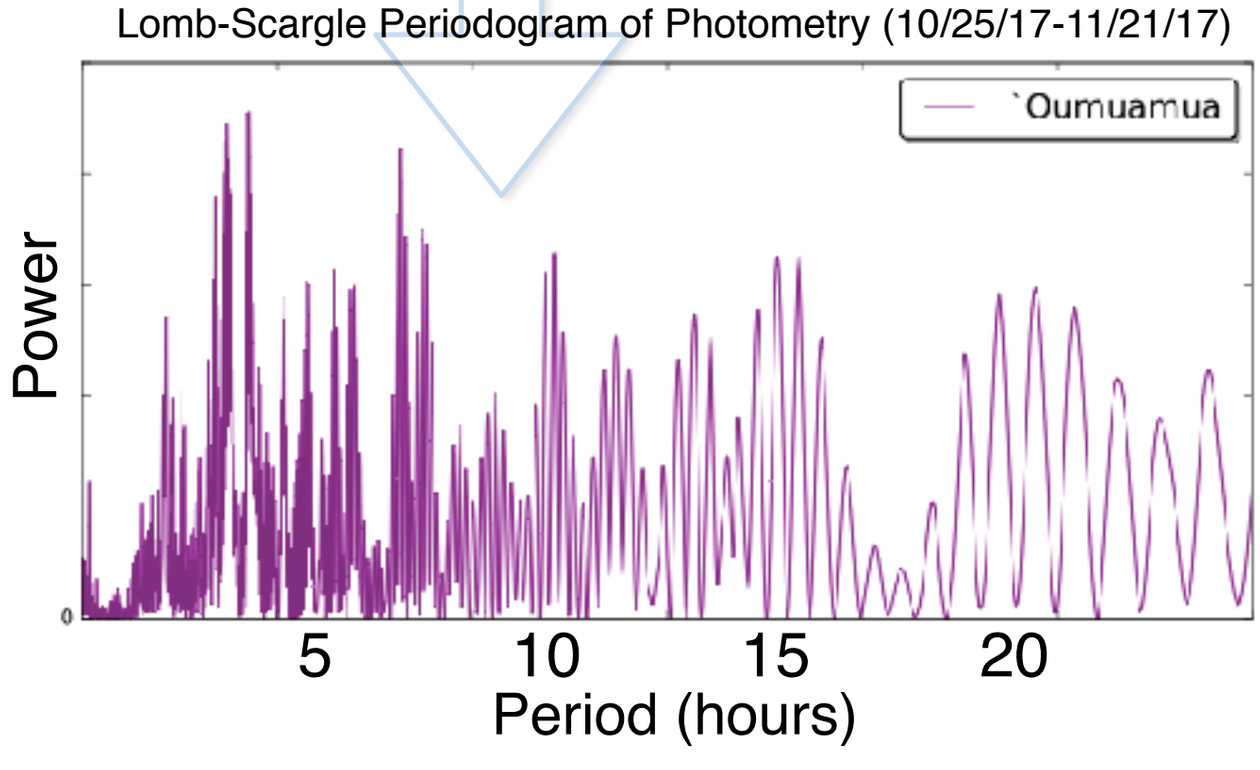

Acceleration

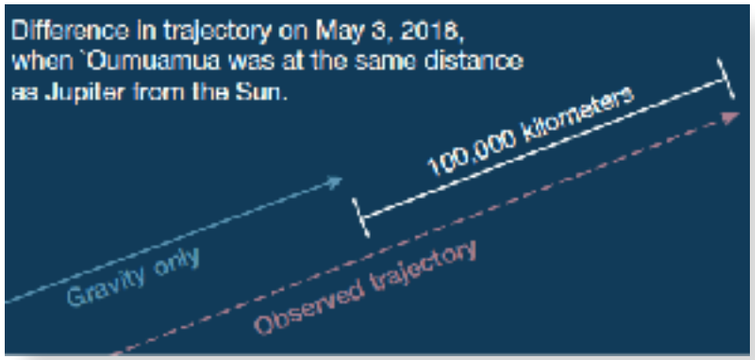

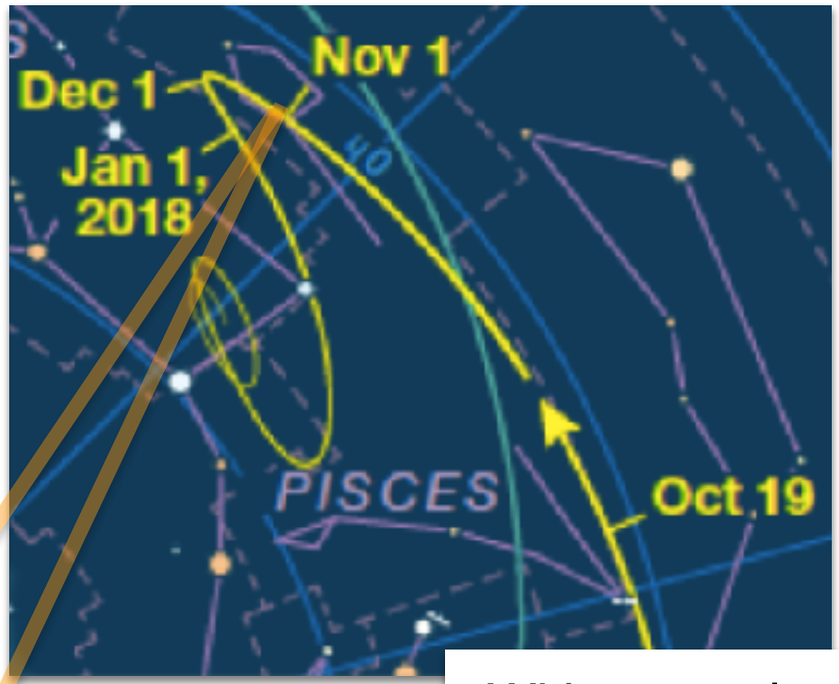

$$\mathbf{a} = 5 \times 10^{-4} \left(\frac{r}{1\,\mathrm{AU}} \right)^{-2} \hat{\mathbf{r}}\ \mathrm{cm\,s^{-2}}$$

Magnitude is about
1/1000th the solar ***g***

Gravity only

With anomalous acceleration term

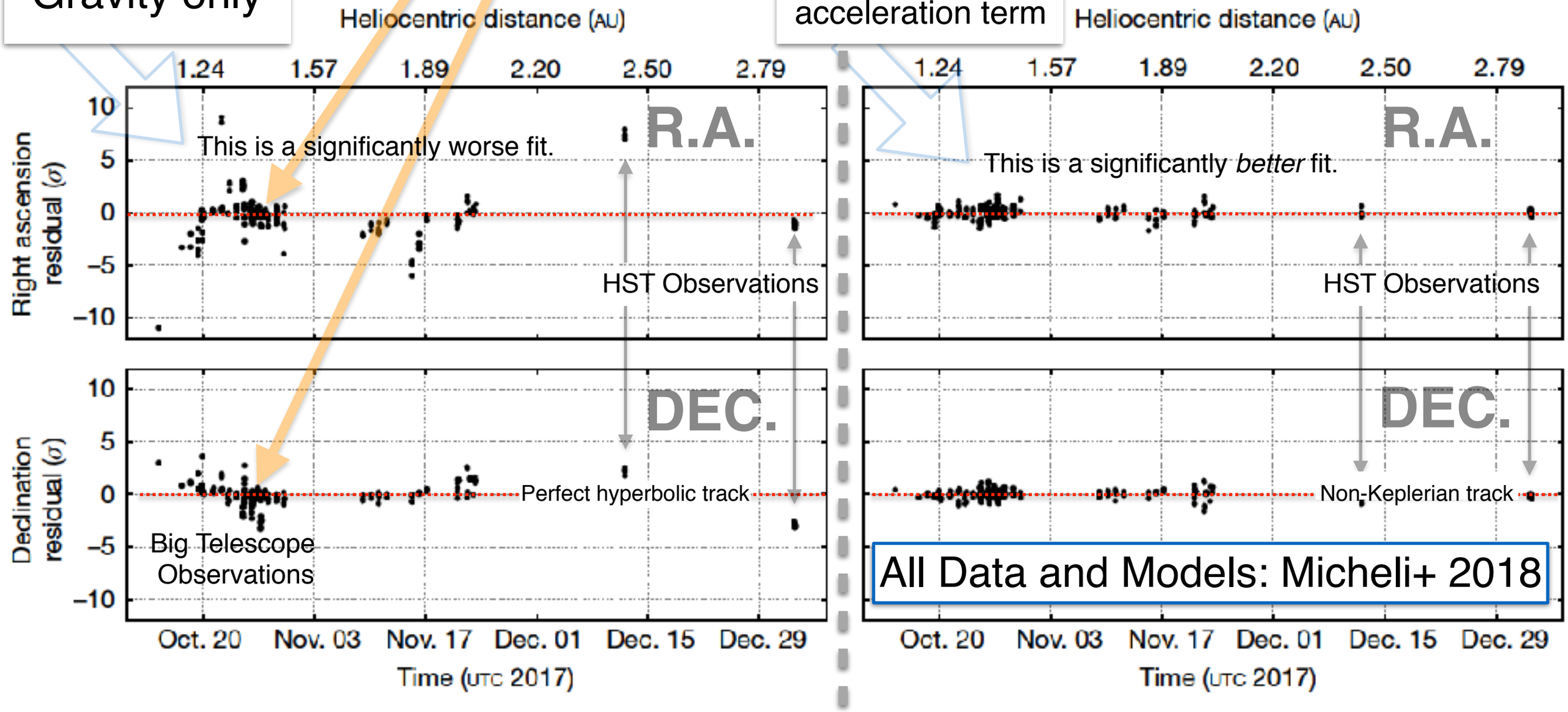

Rigid Body Dynamics

torque from the sun-normal jet

$$\tau(t) = (\xi(t), \eta(t), \zeta(t)) \times \mathbf{F} = A(\xi(t)\hat{\mathbf{j}} - \eta(t)\hat{\mathbf{k}})$$

angular momentum

$$\frac{d}{dt}\mathbf{L}(t) = \tau(t)$$

rotation matrix

$$\frac{d}{dt}\mathbf{R}_i(t) = \left[\mathbf{I}(t)^{-1} \cdot \mathbf{L}(t)\right] \times \mathbf{R}_i(t)$$

moment of inertia tensor (inverse)

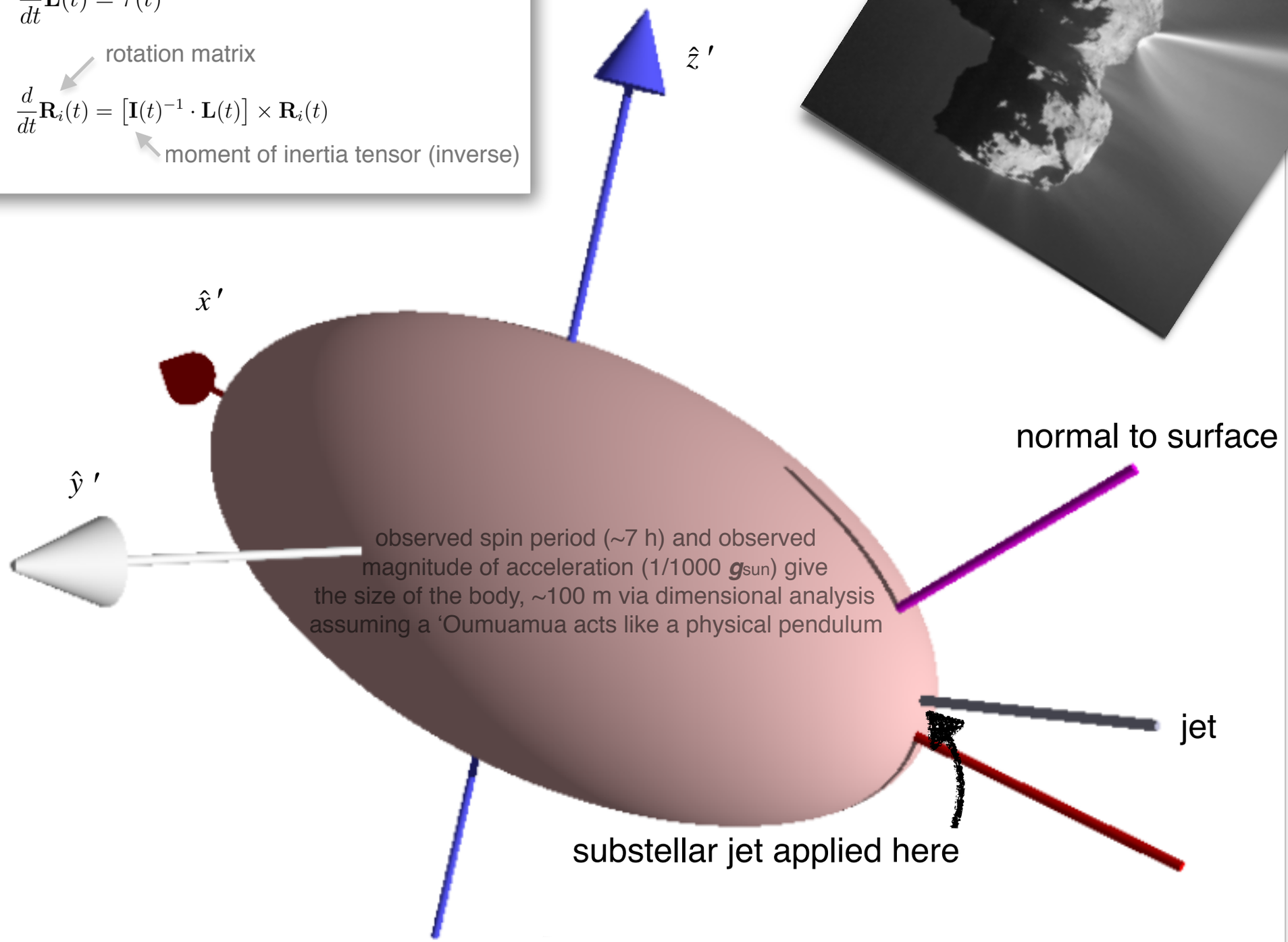

67/P Churyumov-Gerasimenko
ESA-Rosetta

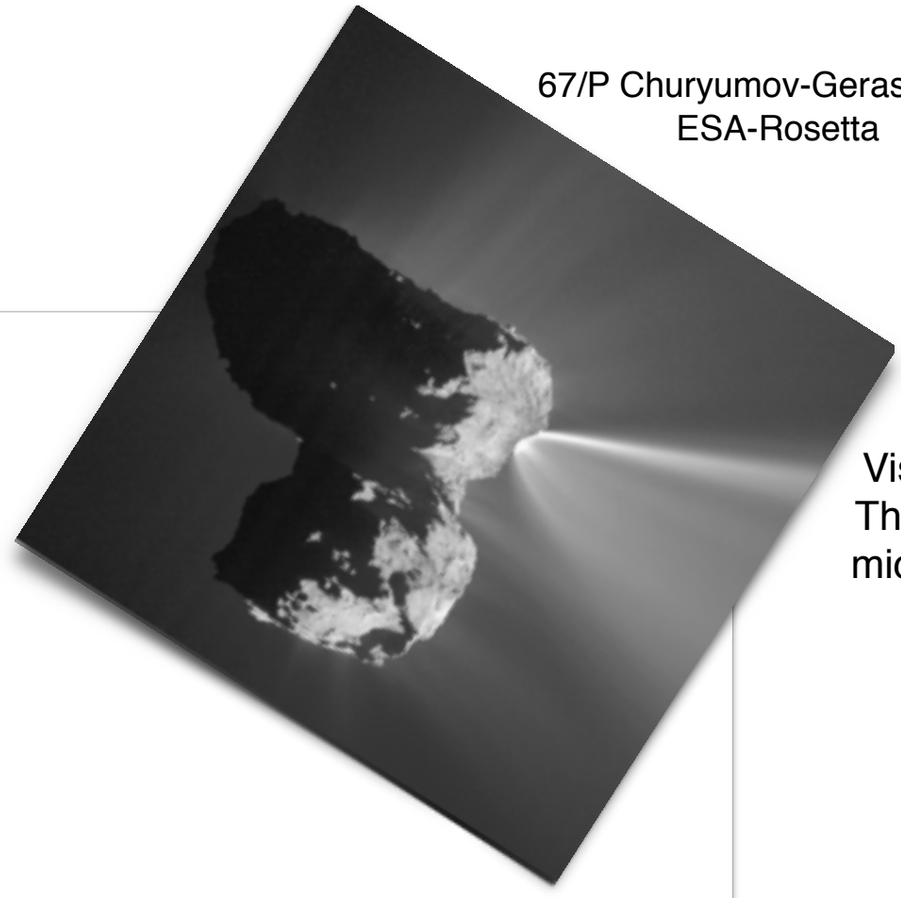

Visible coma…
This jet entrains
micron size dust.

No coma…
This jet can’t entrain
much micron size dust
(or CO).

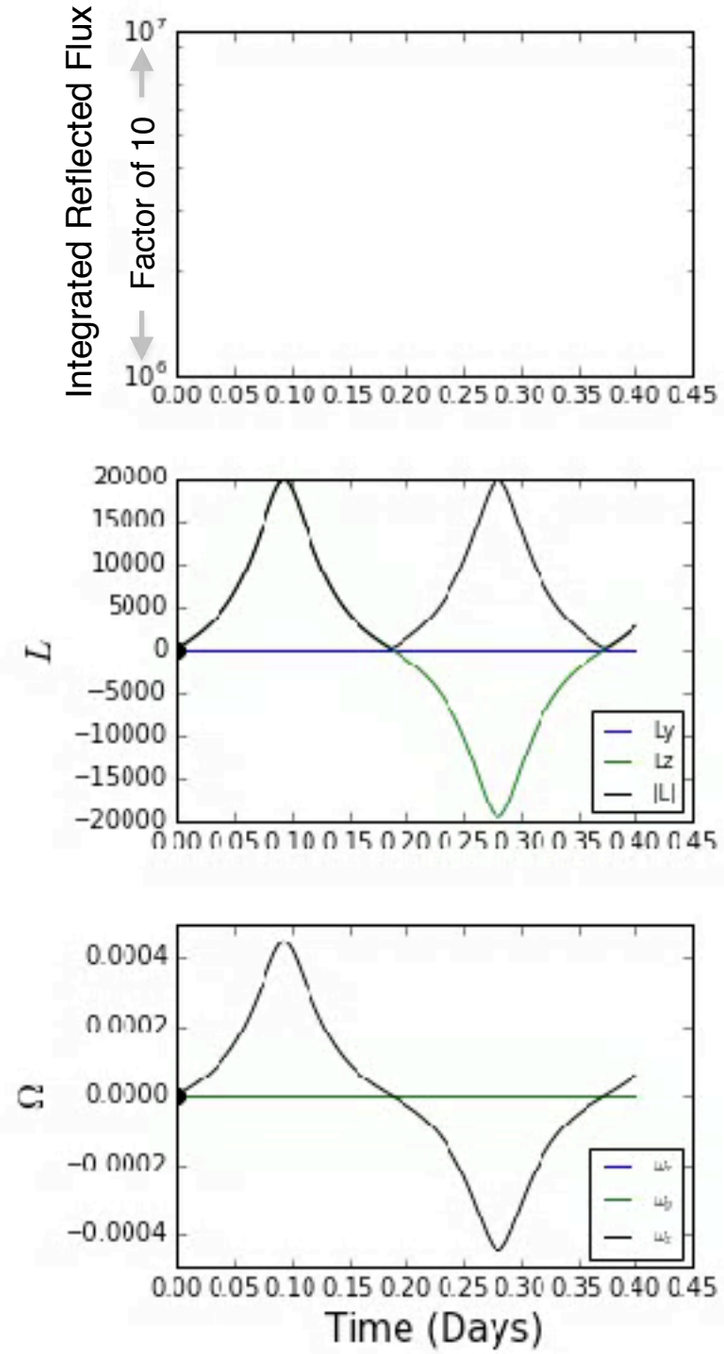

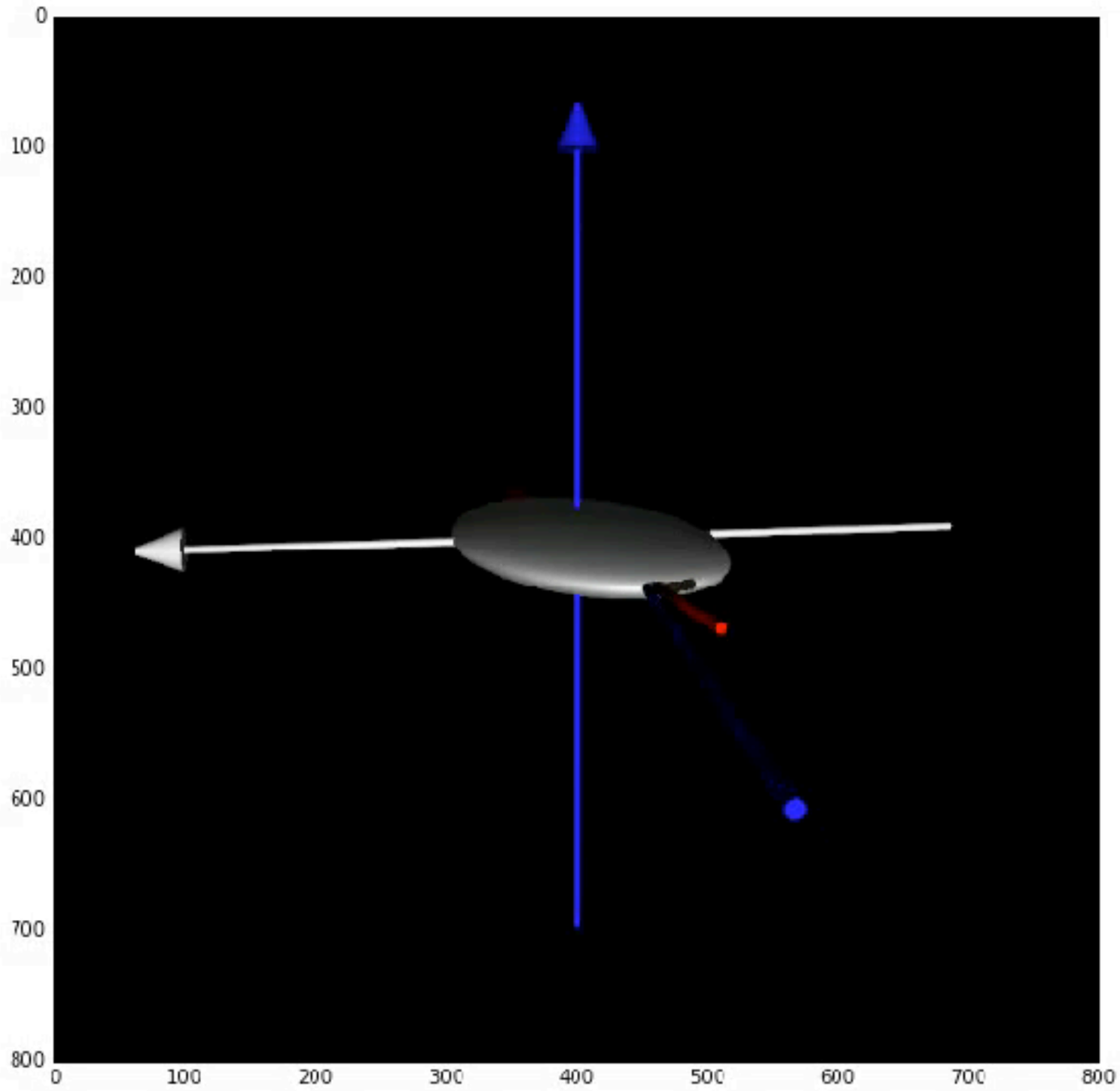

Axes ***not*** included in the photometric model!

Software: POV-Ray

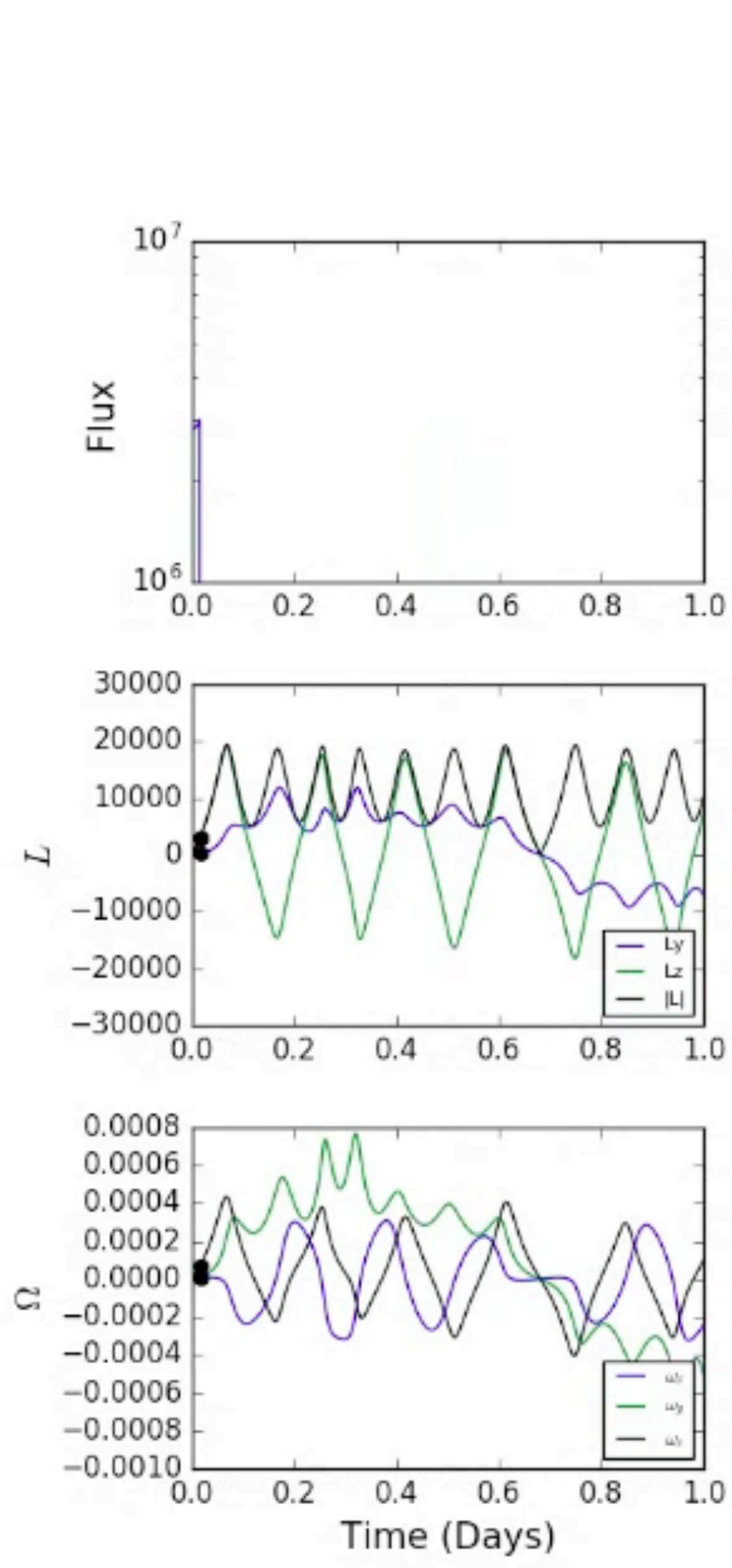
Flux
10^7
10^6
0.0 0.2 0.4 0.6 0.8 1.0
L
30000 20000 10000 0 −10000 −20000 −30000
L_x L_y L_z
Ω
0.0008 0.0006 0.0004 0.0002 0.0000 −0.0002 −0.0004 −0.0006 −0.0008 −0.0010
Time (Days)

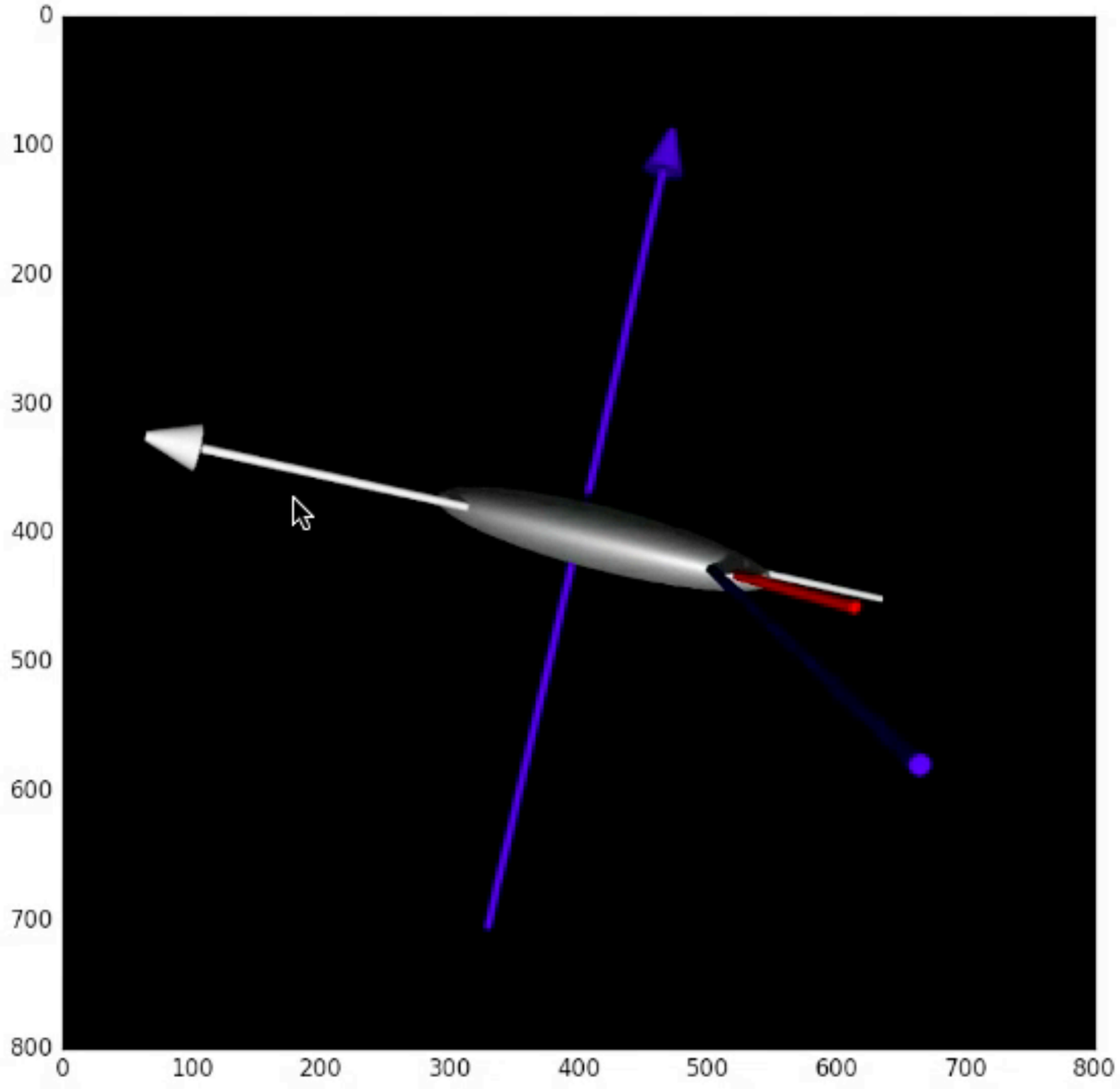
0 100 200 300 400 500 600 700 800

Full light curve modeling

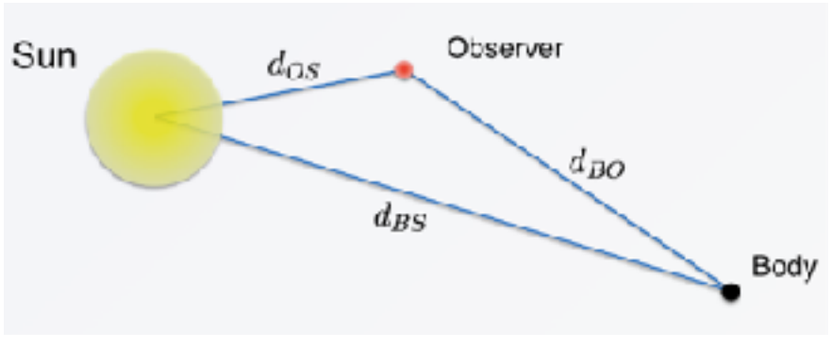

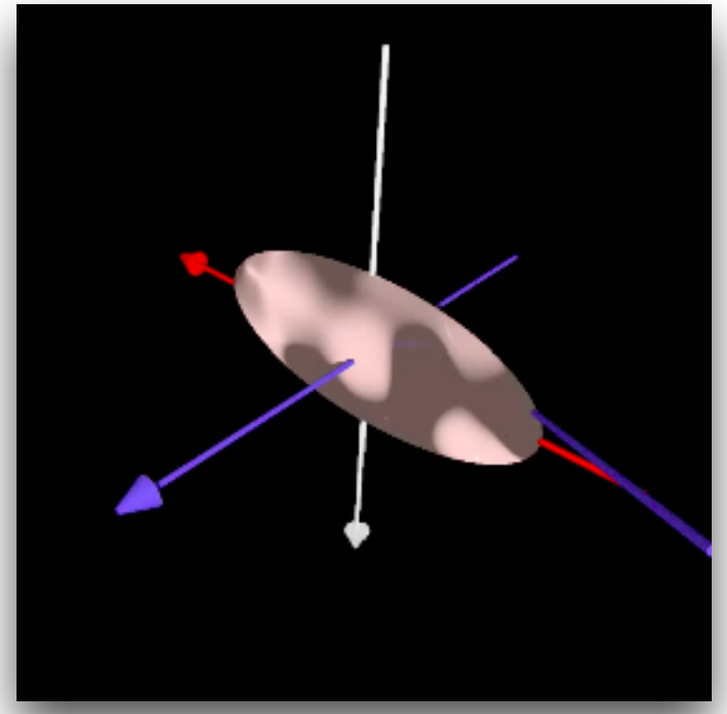

Axes ***not*** included in the photometric model!

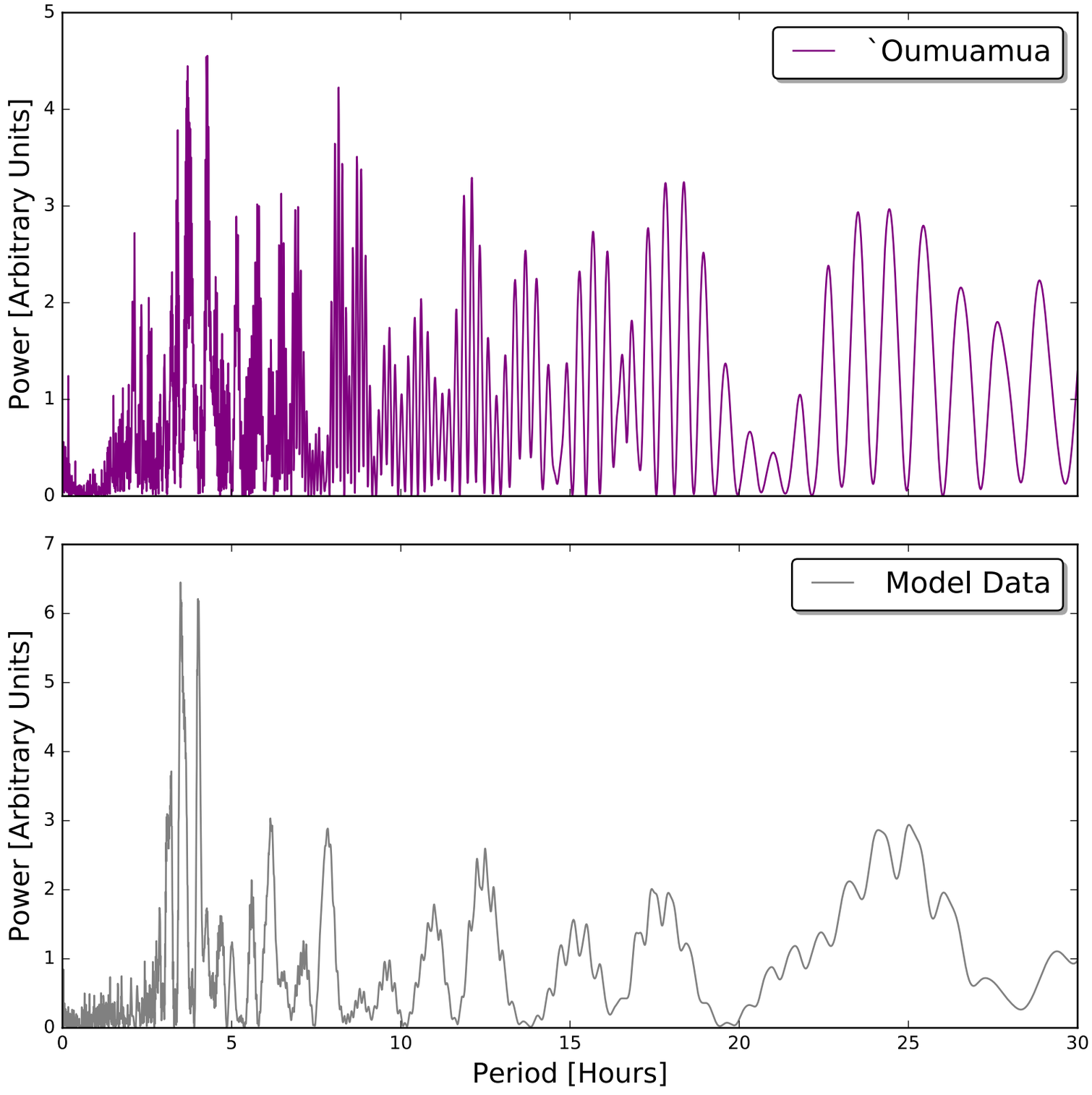

Seligman, Laughlin Batygin — In Preparation

Gravity assist ejects planetesimals

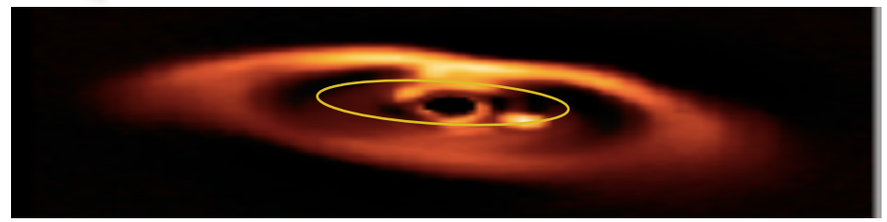
PDS70 —ESO/VLT/SPHERE

In Giant Planet's Frame

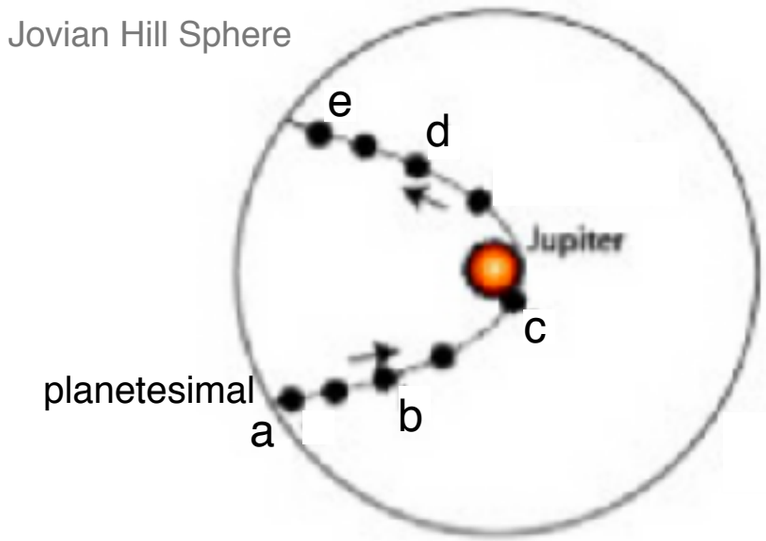

Pan-STARRS detections:

~1/100 AU $^{-3}$

~20 km/s

$$\Gamma = n\sigma v$$

~1/10 event per year

~1 AU ^{2}

$N \sim 10^{26}$ planetesimals

$M \sim 10^{11}$ Earth masses

'Oumuamua-like objects in the Galaxy

In Star's Frame

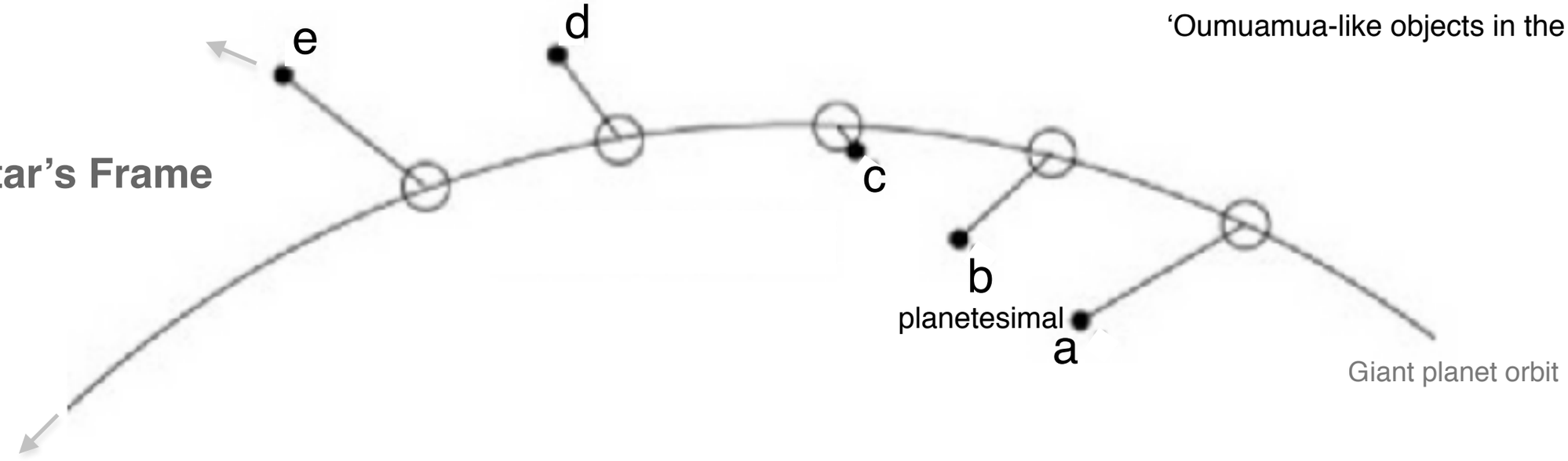

Ejection requires: $v_{\rm esc} = \sqrt{2GM_{\rm P}/R_P} \gtrsim v_{\rm circ} = \sqrt{2GM_\star/a}$

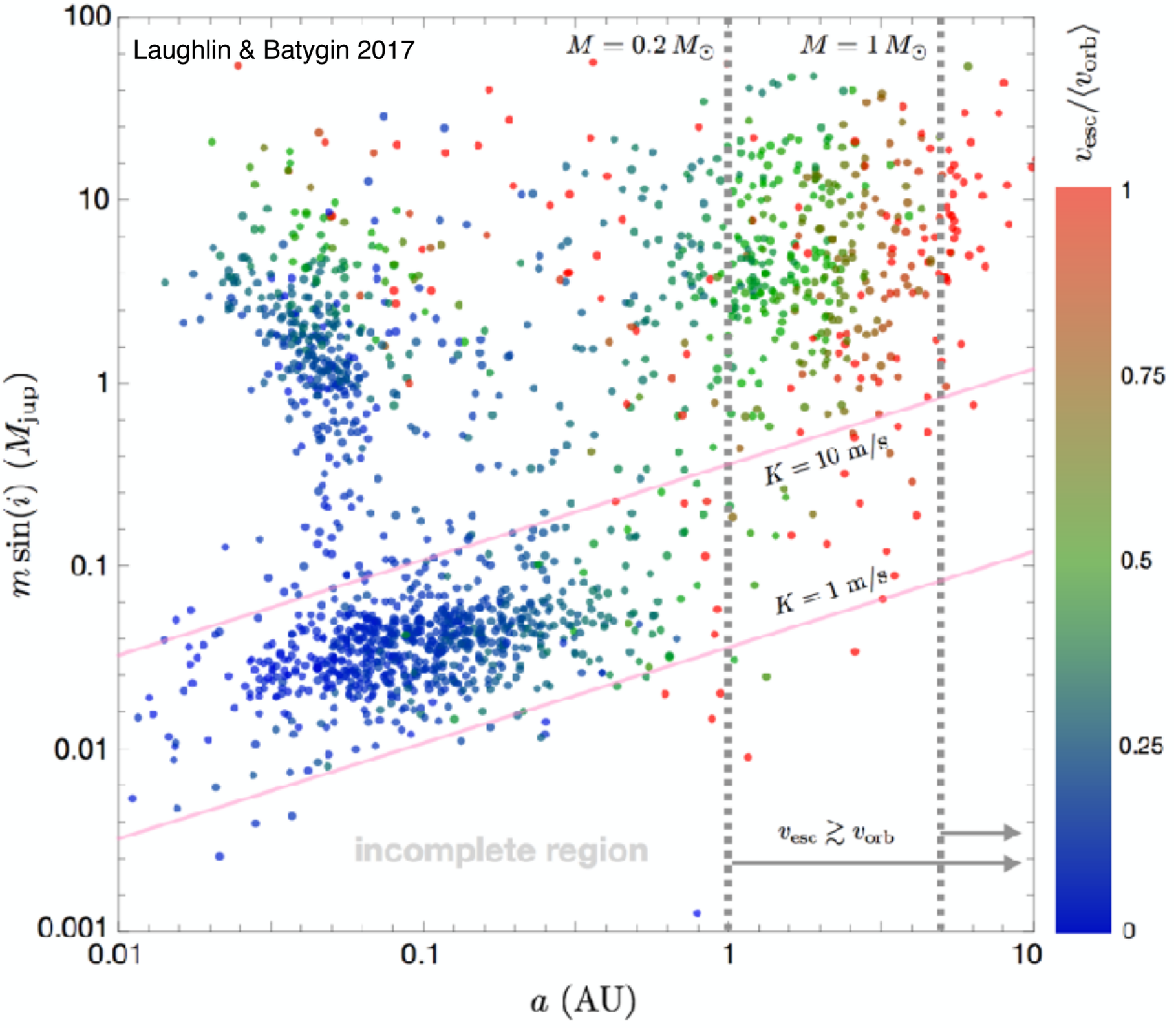

Figure 1. Confirmed extrasolar planets with physical properties drawn from https://exoplanetarchive.ipac.caltech.edu/. Planetary (minimum) mass is shown as a function of the semi-major axis, and the data points are color-coded according to the estimated ratio of the escape velocity and the circular orbital velocity. For objects without direct mass or radius measurements, these quantities are inferred using the linear mass-radius relationship of Wu & Lithwick (2013), with a ceiling of Jupiter radius. In addition to the observations, radial velocity half-amplitudes of $K = 1\,\mathrm{m/s}$ and $K = 10\,\mathrm{m/s}$ are shown for $M = 1 M_\odot$. The interstellar asteroid A/2017 U1 implies a vast and cool, as-yet undetected population of planets with $f = v_{\rm esc}/v_{\rm orb} \gtrsim 1$.

The Disk Substructures at High Angular Resolution Project (DSHARP):
I. Motivation, Sample, Calibration, and Overview

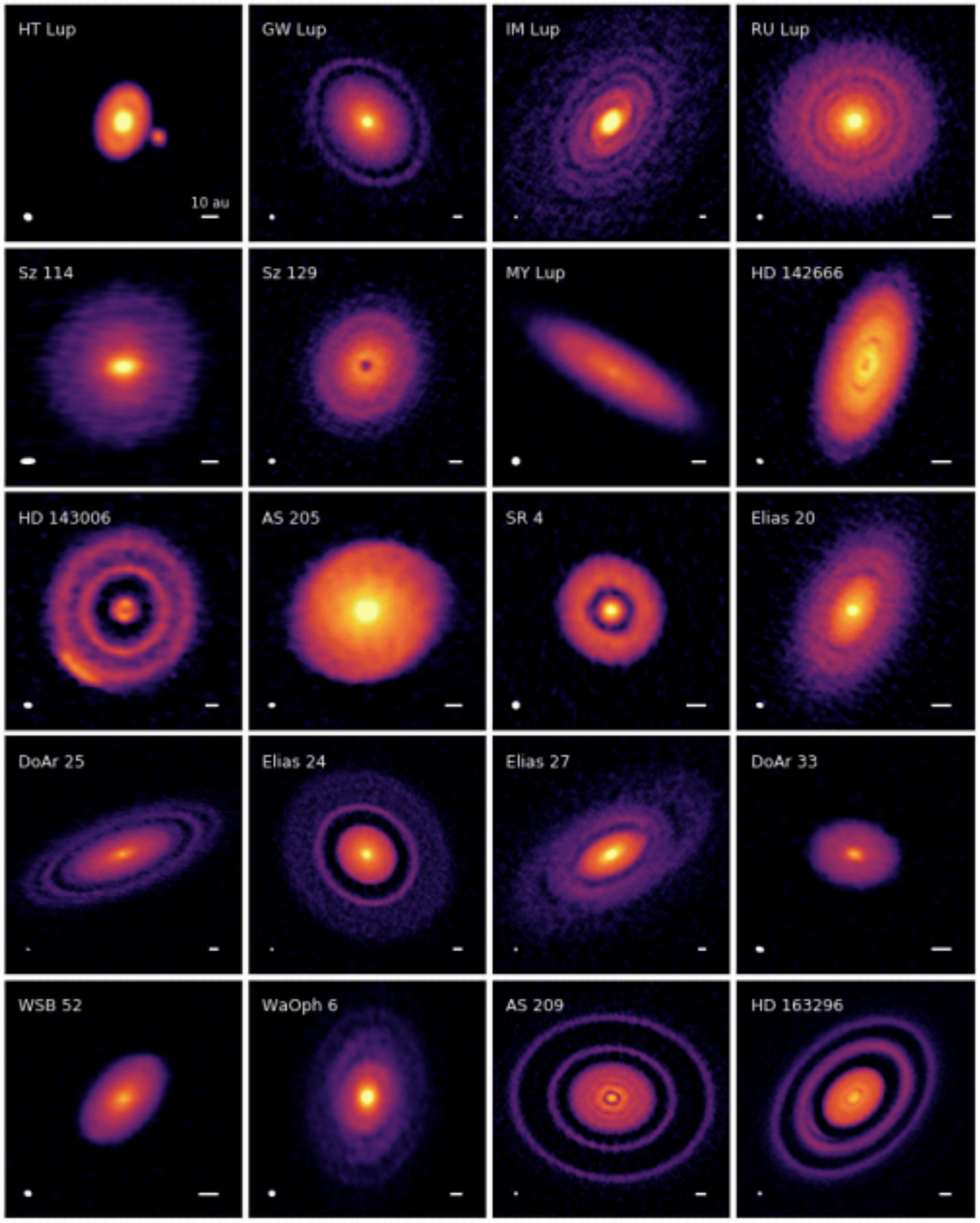

Andrews+ 2018

← Gaps are very common in the disks.

↓

- We plot these potential young planets in the exoplanet mass-semimajor axis diagram (Figure 21). We find that the occurrence rate for $> 5\ M_J$ planets beyond 5-10 au is $\sim 6\%$, consistent with direction imaging constraints. Using disk features, we can probe a planet population which is not accessible by other planet searching techniques. These are Neptune to Jupiter mass planets beyond 10 au. The occurrence rate is $\sim 50\%$, suggesting a flat distribution beyond several au and planets with Neptune mass and above are common. On the other hand, we caution that there are large uncertainties for both the origin of these gaps and the inferred planet mass.

Zhang+ 2018

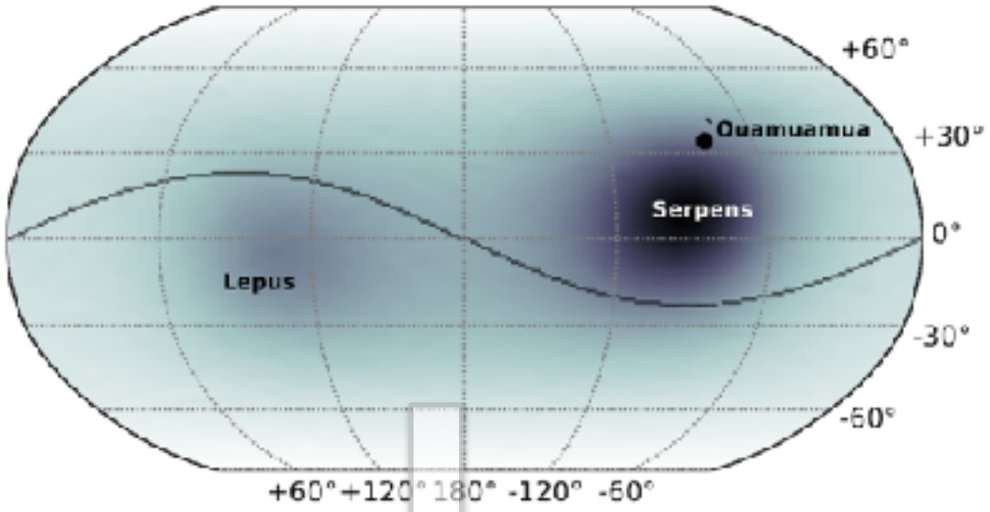

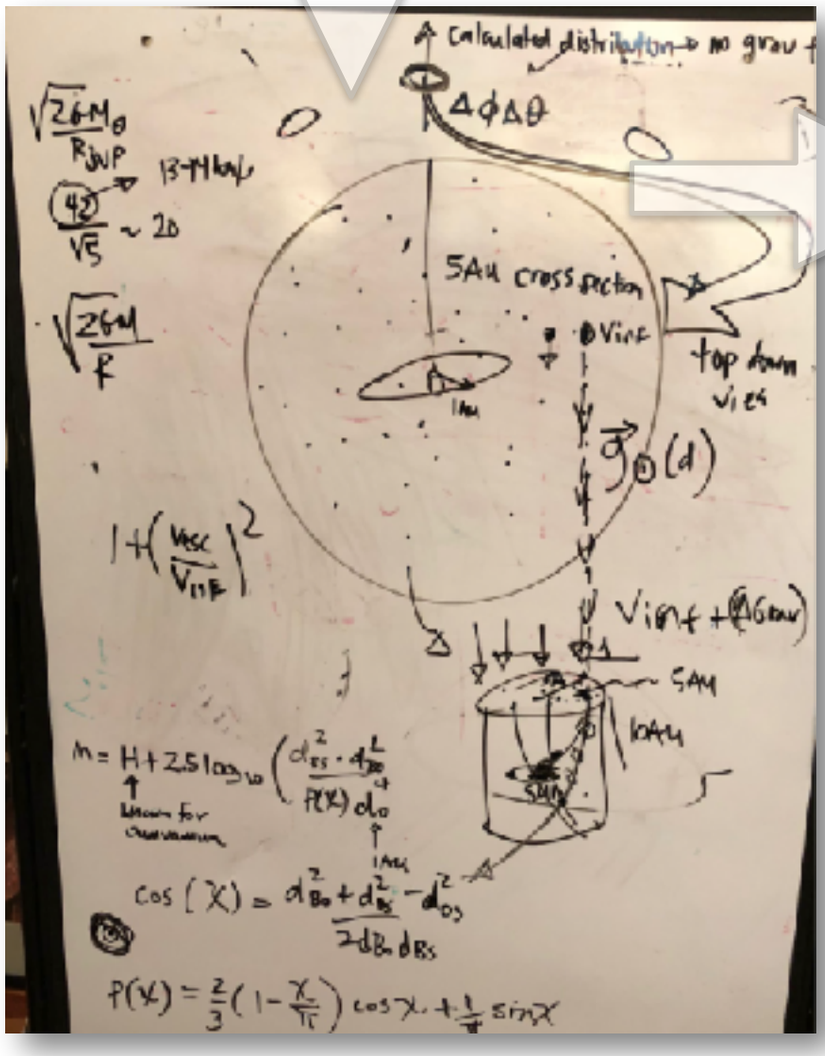

Monte-Carlo Observability Simulations

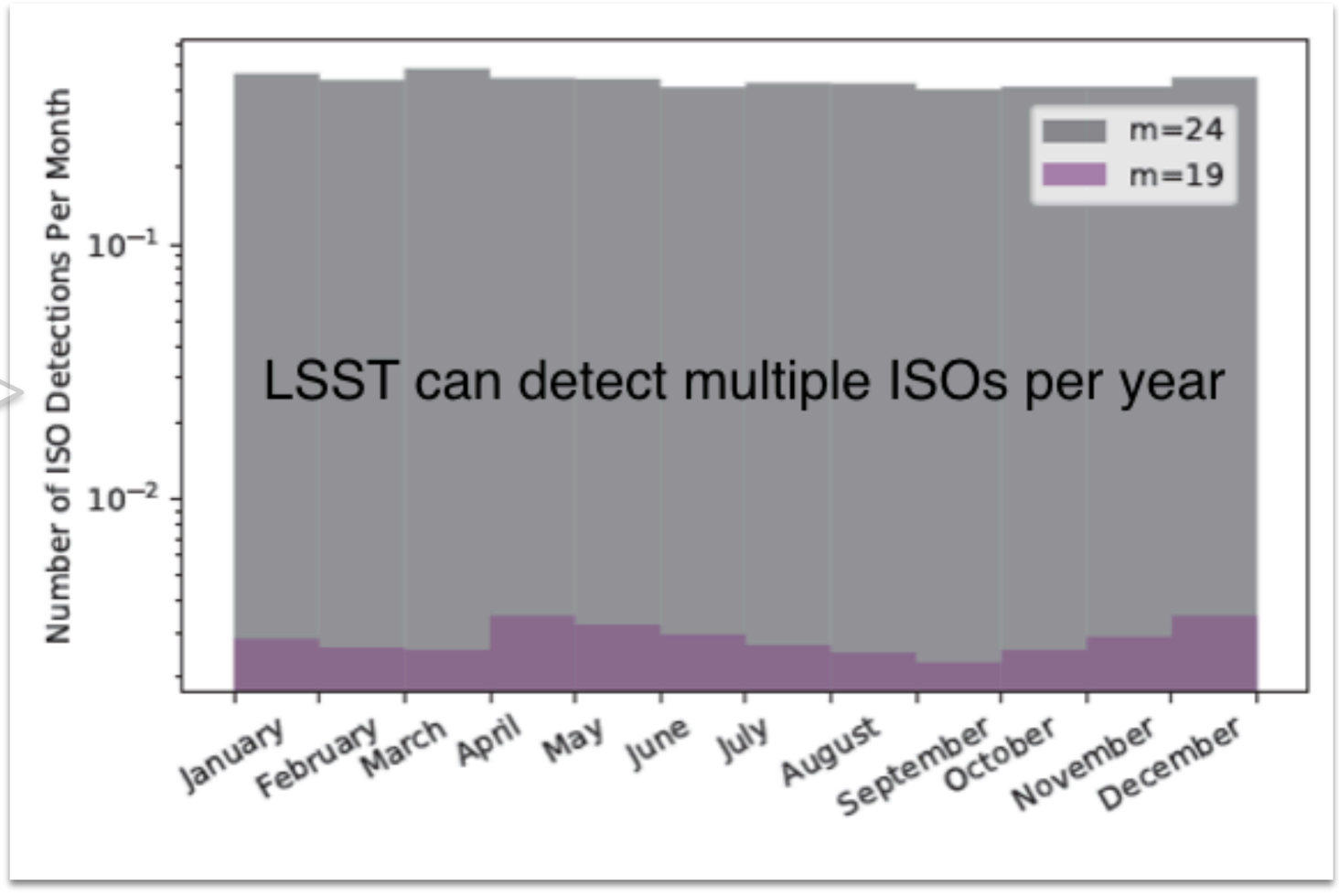

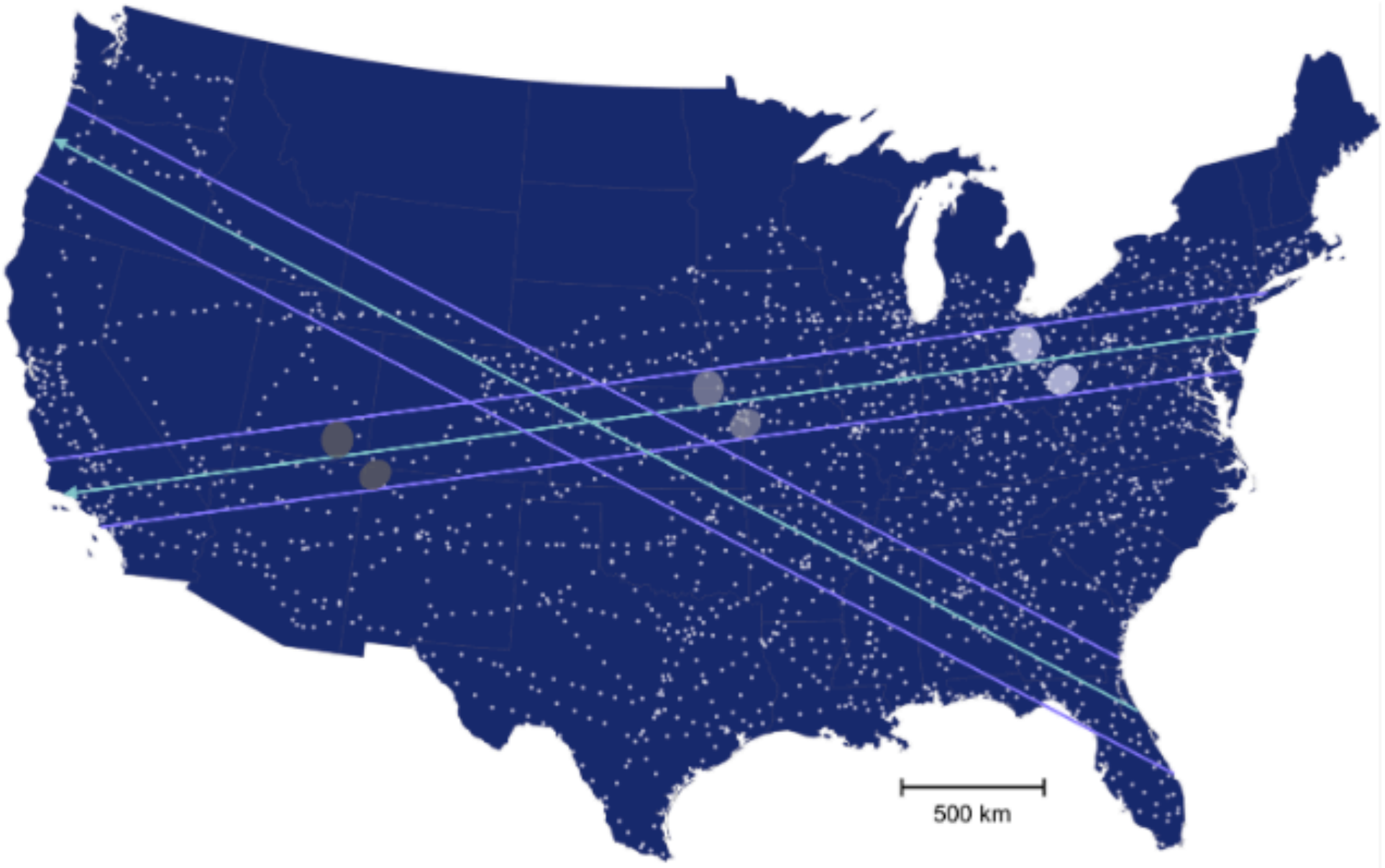

Figure 1. : Schematic of 617 Patroclus-Menoetius occulting the cISP network. Two possible occultation paths are shown to scale, bounded by purple lines with cyan arrows marking the central trajectories. Each white point on the map denotes a cISP network site, where the current cISP network design includes 1913 sites. State boundaries are shown in gray. Relative sizes of the two occulting bodies are based on results from Buie et al. (2015), which reports axial ratios 127 x 117 x 98 km for Patroclus and 117 x 108 x 90 km for Menoetius based on previous stellar occultation measurements.

See talk by Malena Rice in this Meeting.

A Deep-Impact style mission would be a faantastic way to probe an ISO...

SPECIAL SECTION

DEEP IMPACT

RESEARCH ARTICLE

Deep Impact: Excavating Comet Tempel 1

M. F. A'Hearn,[1]* M. J. S. Belton,[2] W. A. Delamere,[3] J. Kissel,[4] K. P. Klaasen,[5] L. A. McFadden,[1] K. J. Meech,[6] H. J. Melosh,[7] P. H. Schultz,[8] J. M. Sunshine,[9] P. C. Thomas,[10] J. Veverka,[10] D. K. Yeomans,[5] M. W. Baca,[9] I. Busko,[11] C. J. Crockett,[1] S. M. Collins,[5] M. Desnoyer,[10] C. A. Eberhardy,[8] C. M. Ernst,[8] T. L. Farnham,[1] L. Feaga,[1] O. Groussin,[1] D. Hampton,[12] S. I. Ipatov,[1] J.-Y. Li,[1] D. Lindler,[13] C. M. Lisse,[1,14] N. Mastrodemos,[5] W. M. Owen Jr.,[5] J. E. Richardson,[7,10] D. D. Wellnitz,[1] R. L. White[11]

Deep Impact collided with comet Tempel 1, excavating a crater controlled by gravity. The comet's outer layer is composed of 1- to 100-micrometer fine particles with negligible strength (<65 pascals). Local gravitational field and average nucleus density (600 kilograms per cubic meter) are estimated from ejecta fallback. Initial ejecta were hot (>1000 kelvins). A large increase in organic material occurred during and after the event, with smaller changes in carbon dioxide relative to water. On approach, the spacecraft observed frequent natural outbursts, a mean radius of 3.0 ± 0.1 kilometers, smooth and rough terrain, scarps, and impact craters. A thermal map indicates a surface in equilibrium with sunlight.

Our knowledge of the interior structure of comets, particularly of the evolution of the outer layers at successive perihelion passages, is almost unconstrained by data and relies instead primarily on theoretical models. Thus, the relation of the coma's composition to the solid composition of the nucleus is uncertain. The Deep Impact (DI) mission, in which a spacecraft would collide with and excavate a cometary nucleus, was conceived, proposed to, and selected by NASA to address this very point (*1*). DI delivered an impact of 19 GJ of kinetic energy to the nucleus of comet 9P/Tempel 1 on 4 July 2005 at about 05:44:36 UT (Earth-received time 05:52:02 UT).

The primary goals of the mission were to determine the differences between the surface of a comet with its ambient outgassing and its interior, which might contain enhanced volatiles, and to determine the structural properties and strength of the surface layers.

DI consisted of two fully functional spacecraft: an impacting spacecraft weighing 364 kg (plus 6.5 kg of unused hydrazine fuel, N_2H_4, at time of impact) and a flyby spacecraft for observing the impact and relaying data from the impactor. The impactor used an autonavigation system to analyze images of the comet and target the impactor at a site on the nucleus that would be in sunlight and visible from the flyby spacecraft. Impact speed was 10.3 km/s. The impactor was 49% copper to minimize chemical reactions with water in the comet that would lead to bright emission features. The two spacecraft separated 24 hours before impact, at which point the flyby spacecraft diverted to miss the nucleus by 500 km and slowed down by 100 m/s to provide an 800-s viewing window after impact. At 500 km before closest approach, the flyby spacecraft froze in an attitude that kept its dust shields in the proper orientation. After passing through the innermost coma, the spacecraft turned and looked back at the comet to take additional data (*2*, *3*). The event was also recorded at nearly all the world's remote observing facilities, both ground-based and space-based, to provide more extensive coverage in both time and space than was possible from a flyby mission (*4*).

[1]University of Maryland, College Park, MD 20742, USA. [2]Belton Space Exploration Initiatives, Tucson, AZ 85716, USA. [3]Delamere Support Services, Boulder, CO 80301, USA. [4]Max-Planck-Institute for Solar System Research, Katlenburg-Lindau, D37191 Germany. [5]Jet Propulsion Laboratory, Pasadena, CA 91109, USA. [6]University of Hawaii, Honolulu, HI 96822, USA. [7]University of Arizona, Tucson, AZ 85721, USA. [8]Brown University, Providence, RI 02912, USA. [9]SAIC, Chantilly, VA 20151, USA. [10]Cornell University, Ithaca, NY 14853, USA. [11]Space Telescope Science Institute, Baltimore, MD 21218, USA. [12]Ball Aerospace and Technology Corporation, Boulder, CO 80301, USA. [13]Sigma Scientific, Greenbelt, MD 20771, USA. [14]Applied Physics Laboratory, Johns Hopkins University, Laurel, MD 20723, USA.

*To whom correspondence should be addressed. E-mail: ma@astro.umd.edu

The Comet Before Impact

The nucleus. The comet was observed by the flyby spacecraft almost continuously from several days before impact until impact and at 4-hour intervals for weeks before the nearly continuous observing. In addition, the impactor obtained images beginning shortly after release from the flyby until ~4 s before impact. The only comet that has been comparably well studied is comet Halley at its 1986 apparition. Figure 1 shows a composite of several images from the impactor, with the highest resolution in the vicinity of the impact site.

The shape of the nucleus is incompletely determined because the slow rotation period, 40.7 hours, and the high velocity of the flyby resulted in only slightly more than half the surface being illuminated and resolved. However, the nucleus was in full silhouette after the flyby, backlit by ejecta from the impact, which strongly constrains the mean radius. Images from the medium resolution instrument (MRI) covered ~25% of the object with sufficient stereo convergence and resolution to solve for 70 control points in 43 images, with an average relative uncertainty of <30 m. The positive spin pole was determined to be within 10° of RA = 5°, Dec = 78°. This solution compares favorably with a pre-encounter measurement of RA = 46°, Dec = 73° based on light curve analysis (*5*). The spin vector was constrained by the projected spin axis found in approach images, combined with matching outlines of the body in images before and after the encounter.

The control points, in combination with limb outlines, restrict the shape for slightly more than half the area, but some longitudes remain unobserved. The mean radius of the model is estimated to have been 3.0 ± 0.1 km in

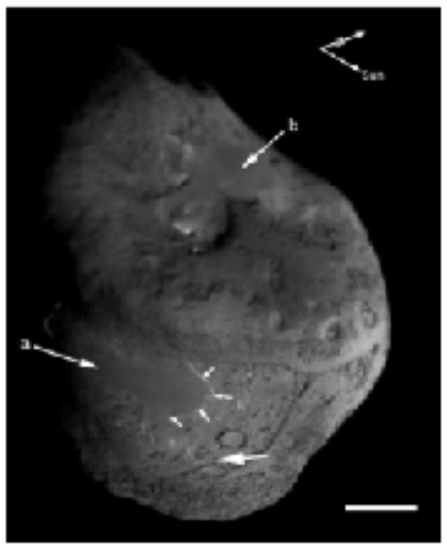

Fig. 1. Composite of ITS images. The Sun is to the right and celestial north is toward the upper right, near the rotational pole. Ecliptic north is another 20° counterclockwise from the north pole. Arrows a and b point to the large, smooth areas. The impact site is indicated by the other large arrow. The small arrows highlight the scarp, bright due to the illumination angle, which shows the smooth area to be elevated above the extremely rough terrain. The scale bar is 1 km, and the two arrows above the nucleus point to the Sun and to the rotational axis of the nucleus. Celestial north is near the rotational pole; ecliptic north is more nearly upward.

Oumuamua would have readily interceptible given advance warning

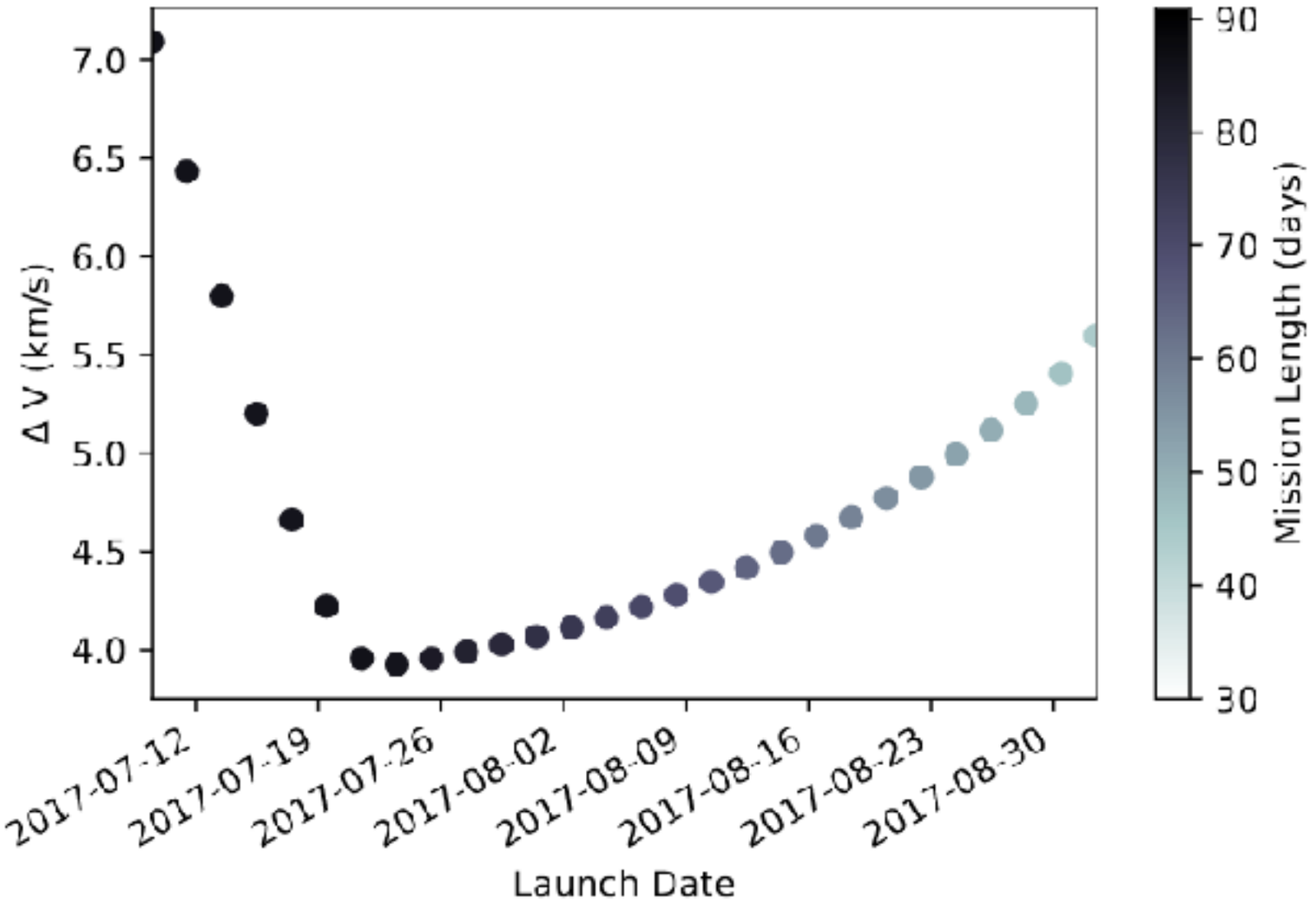

FIG. 5.—: Optimal flight ΔV's as a function of launch date during the mid-2017 launch window for 'Oumuamua interception trajectories. The x-axis shows the launch date and the y-axis shows the minimum required impulsive change in velocity (relative to Earth's orbit, with Earth treated as a test particle) to intercept 'Oumuamua. Each launch opportunity is shaded by the time of flight required for the minimum-energy trajectory. The color-bar on the right is shown in units of days. As a rule of thumb, the minimum energy trajectories lead to impact with the target as it reaches its closest approach to the Earth.

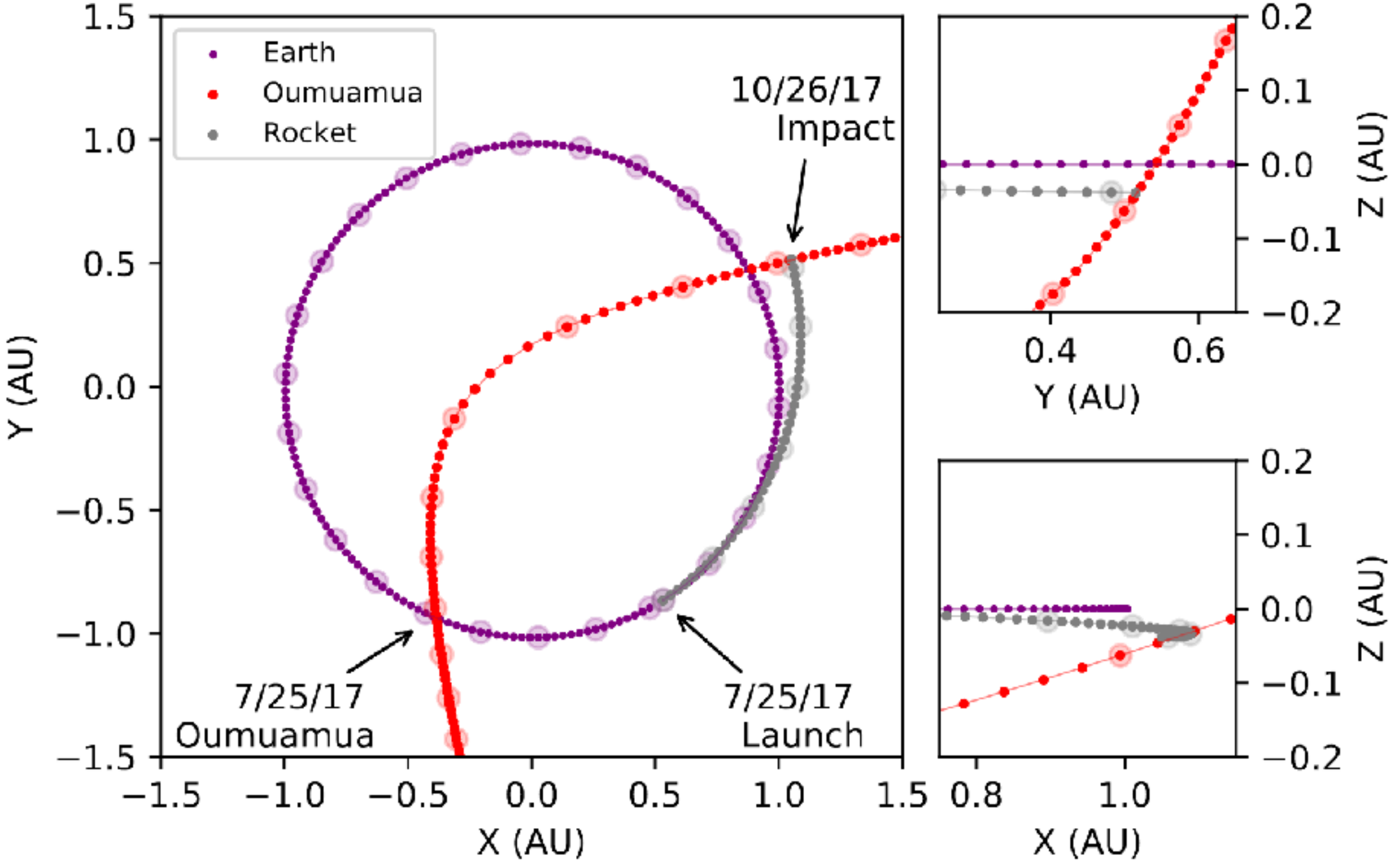

FIG. 6.—: Trajectory of an optimal interception mission sent on July 25th 2017. The trajectories for 'Oumuamua, the Earth, and the rocket are plotted in blue, black and grey respectively in four day intervals in the smaller circles. The larger circles are plotted in 28 day intervals.

2014 MU69 last week

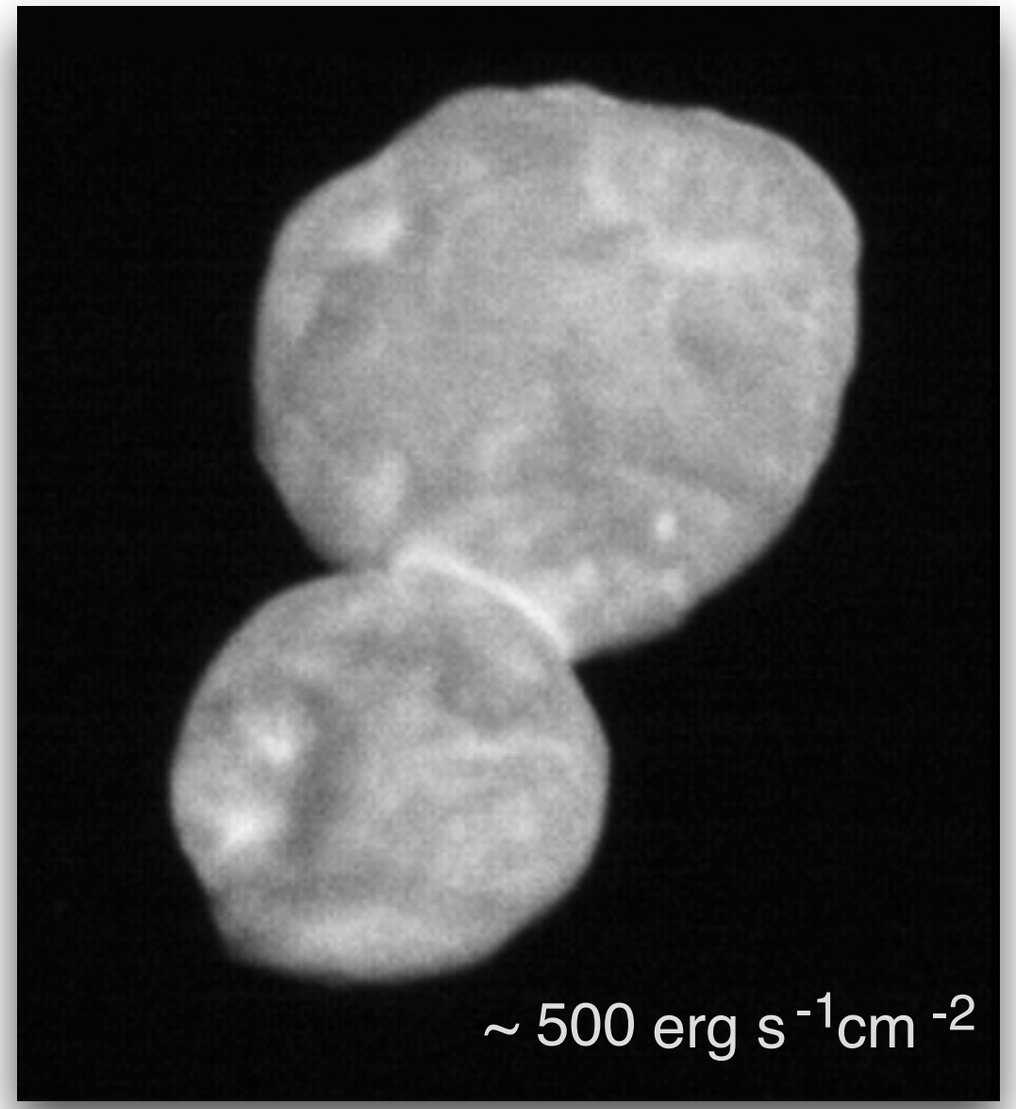

2014 MU69 7 Gyr from now

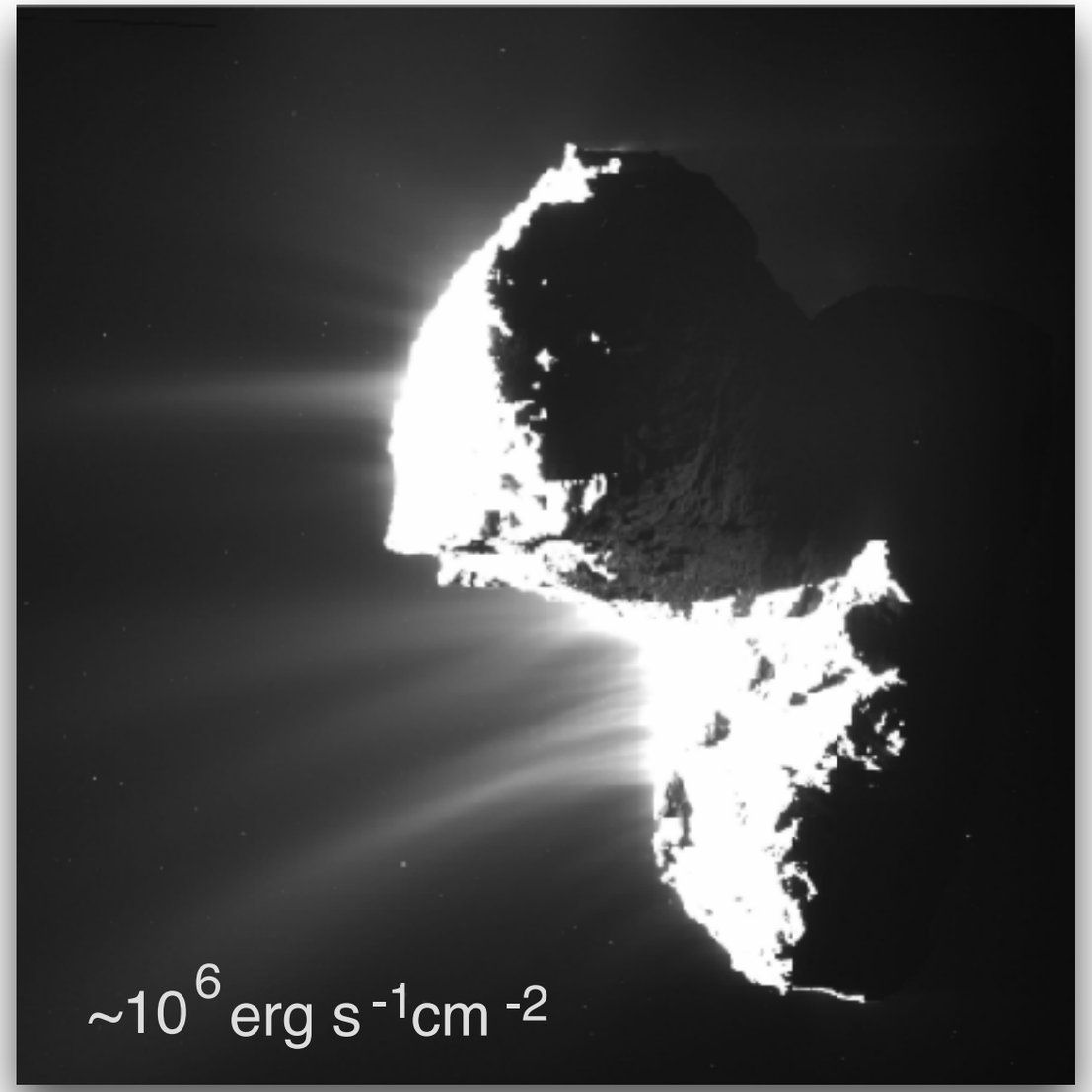

Oumuamua, however, will chill out for the duration. To very high likelihood, it will never have another close encounter with a main-sequence star.

First Results from a Superconductive Detector for Moving Magnetic Monopoles

Blas Cabrera
Physics Department, Stanford University, Stanford, California 94305
(Received 5 April 1982)

A velocity- and mass-independent search for moving magnetic monopoles is being performed by continuously monitoring the current in a 20-cm^2-area superconducting loop. A single candidate event, consistent with one Dirac unit of magnetic charge, has been detected during five runs totaling 151 days. These data set an upper limit of 6.1×10^{-10} cm^{-2} sec^{-1} sr^{-1} for magnetically charged particles moving through the earth's surface.

PACS numbers: 14.80.Hv

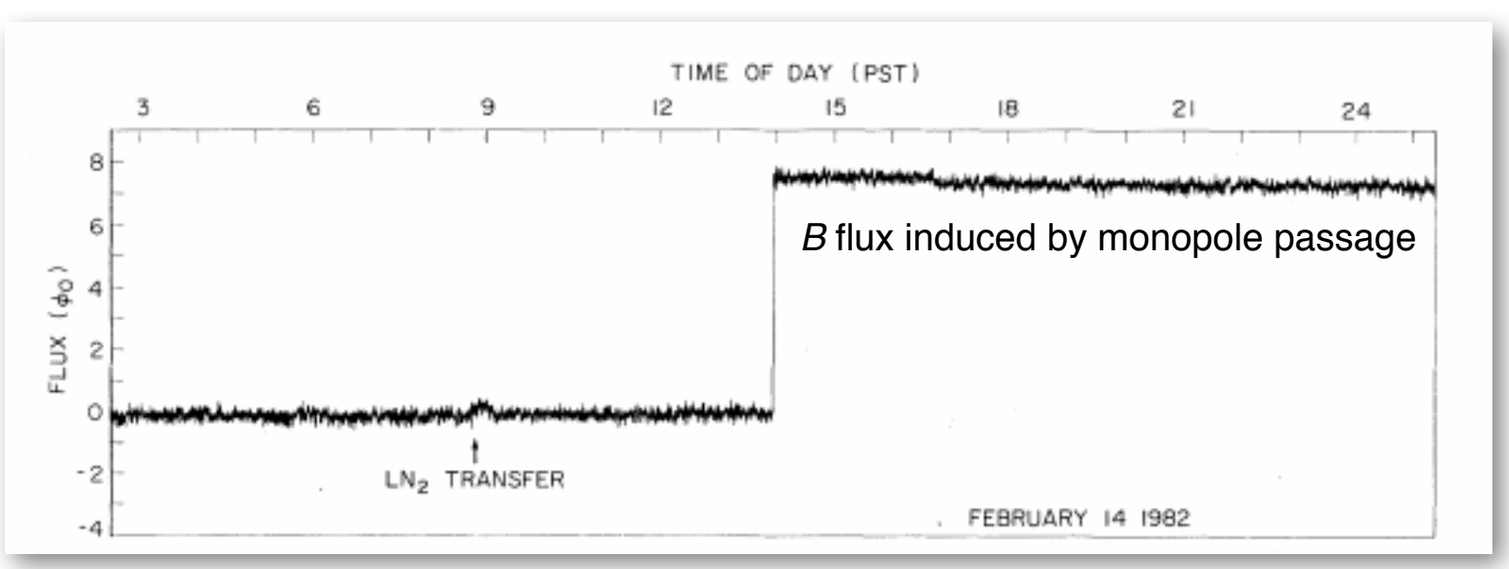

B flux induced by monopole passage

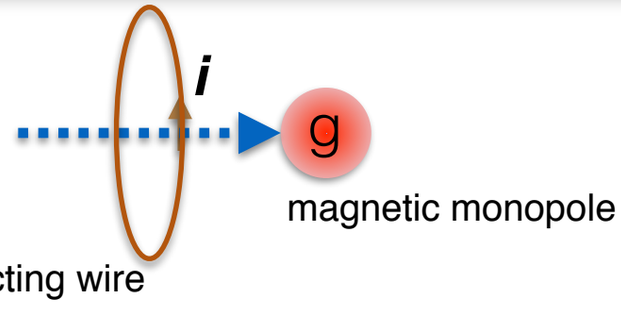

magnetic monopole

superconducting wire

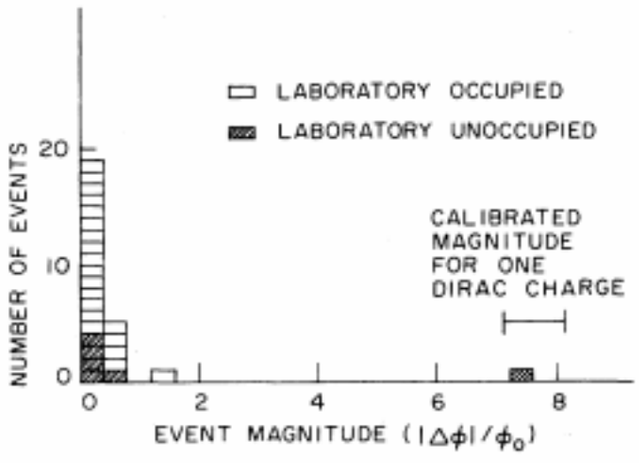

FIG. 3. Histogram of all event magnitudes.

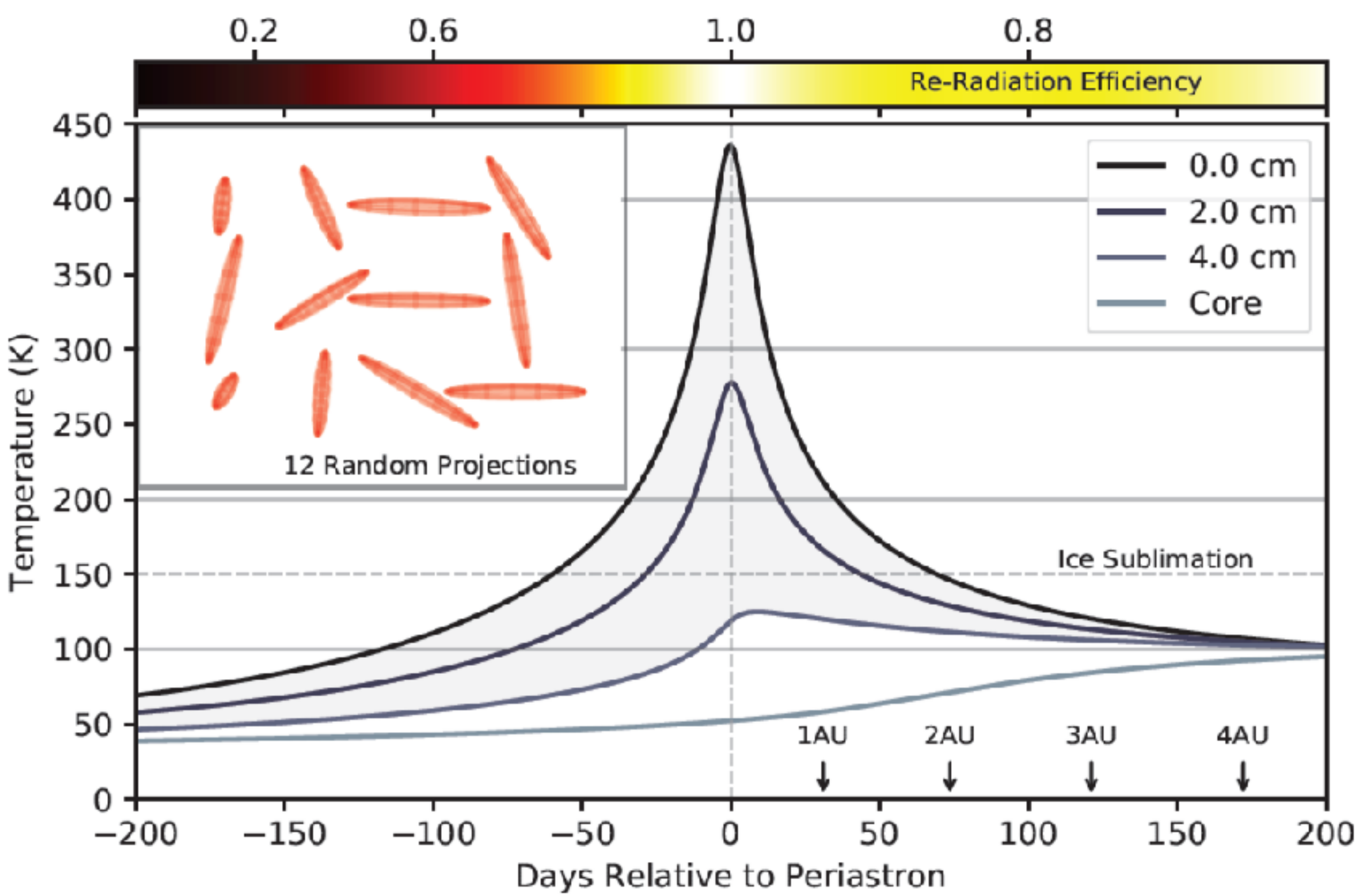

FIG. 1.—: Thermal modeling of 'Oumuamua during its solar encounter. We show the temperature profile at depths of 0.0, 2.0, 4.0 cm (the regolith-ice interface) and at the center over the 200 days prior to and after periastron. The upper left inset shows twelve different projections of a 10:1:1 triaxial ellipsoid defined by random rotations though the first two Euler angles, to provide a visual depiction of the small average projected surface area, due to 'Oumuamua's chaotic tumbling, see Eqn. 12. The top panel shows the efficiency of blackbody radiation during the flyby, evaluated as the instantaneous energy radiated/energy received. In the simulation, the icy asteroid is coated in a 4cm thick layer of porous regolith material, as indicated by the shading, and we use thermal properties typical of such materials. We verify that globally, energy in the simulation is conserved to better than a factor of $\sim 1\%$ of the cumulative sum of the total energy received minus the total radiated, using a Bond albedo of $\alpha = .01$ and bolometric emissivity of $\epsilon = .95$. The arrows indicate the times where 'Oumuamua reaches distances of 1, 2, 3 and 4 AU from the Sun as it exits the Solar System. It is evident that with this choice of depth and conductivity, 'Oumuamua never produces a visible coma.